JOURNAL OF GEOPHYSICAL RESEARCH, VOL. 108, NO. D1, 4008, doi:10.1029/2001JD001543, 2003

A semianalytical cloud retrieval algorithm using backscattered radiation in 0.4–2.4 μm spectral region

A. A. Kokhanovsky,[1,2] V. V. Rozanov,[1] E. P. Zege,[2] H. Bovensmann,[1] and J. P. Burrows[1]

Received 26 November 2001; revised 23 May 2002; accepted 25 June 2002; published 8 January 2003.

[1] This study is devoted to the development of a semianalytical algorithm for the determination of the optical thickness, the liquid water path, and the effective size of droplets from spectral measurements of the intensity of light reflected from water clouds with large optical thickness. The probability of photon absorption by droplets in the visible and near-infrared spectral regions is low. This allows us to simplify and modify well-known asymptotic equations of the radiative transfer theory, taking into account the fact that the single scattering albedo is close to one. Modified asymptotic equations are used to develop the inverse algorithm. We also avoid the use of the Mie theory, applying parametrizations and geometrical optics results with account for wave corrections. The main advantage of the method proposed lays in the fact that the equations derived not only provide a valuable alternative to the numerical radiative transfer solution but also are much more simple than equations of a conventional asymptotic theory. This simplicity allows both the simplification of the cloud retrieval algorithm and, even more important, the insight into various factors involved in a retrieval scheme. *INDEX TERMS:* 3360 Meteorology and Atmospheric Dynamics: Remote sensing; 3367 Meteorology and Atmospheric Dynamics: Theoretical modeling; 3359 Meteorology and Atmospheric Dynamics: Radiative processes; *KEYWORDS:* radiative transfer, clouds, light scattering

Citation: Kokhanovsky, A. A., V. V. Rozanov, E. P. Zege, H. Bovensmann, and J. P. Burrows, A semianalytical cloud retrieval algorithm using backscattered radiation in 0.4–2.4 μm spectral region, *J. Geophys. Res.*, *108*(D1), 4008, doi:10.1029/2001JD001543, 2003.

1. Introduction

[2] Clouds play an important role in the Earth climate system [*Kondratyev and Binenko*, 1984; *Liou*, 1992]. The amount of radiation reflected by the Earth-atmosphere system into outer space does not only depend on the cloud cover and the total amount of condensed water in the Earth atmosphere. The size of droplets or crystals a_{ef} is also of importance.

[3] The information about microphysical properties and spatial distributions of terrestrial clouds on a global scale can be achieved with satellite remote sensing systems only. Different spectrometers and radiometers [*Bovensmann et al.*, 1999; *Deschamps et al.*, 1994; *King et al.*, 1992; *Nakajima et al.*, 1998], deployed on space-based platforms, measure the angular and spectral distribution of intensity and polarization of the reflected solar light. Generally, the measured values depend on both geometrical and microphysical characteristics of clouds. Thus, the inherent properties of clouds can be retrieved (at least in principle) by solution of the inverse problem. The accuracy of the retrieved values depends on the accuracy of measurements and the accuracy of the forward radiative transfer model.

[4] In particular, it is often assumed that clouds can be represented by homogeneous and infinitely extended, in the horizontal direction plane-parallel slabs [*Goloub et al.*, 2000; *Han et al.*, 1994; *King*, 1981, 1987; *Nakajima and King*, 1990; *Nakajima et al.*, 1991; *Rossow*, 1989]. The range of applicability of such an assumption for real clouds is very limited as is readily shown by observations of light from the sky on the cloudy day. For example, the retrieved cloud optical thickness τ apparently depends on the viewing geometry [*Loeb and Davies*, 1996; *Loeb and Coakley*, 1998]. This, of course, would not be the case for an idealized plane-parallel cloud layer. However, the state-of-the-art radiative transfer theory and computer technology do not allow one to incorporate 3D effects into operational satellite retrieval schemes. As a result, cloud parameters retrieved should be currently considered as a rather coarse approximation to reality. This justifies the development of new cloud retrieval algorithms, which can in principle have a lower accuracy than exact radiative transfer models, if one applies them to simulated radiance fields. However, they may yield very similar accuracies, when applied to real data. This is due to uncertainties of forward models for real atmospheres.

[5] Note that even such limited tools produce valuable information on terrestrial clouds properties. For example, it was confirmed by satellite measurements that droplets in clouds over oceans are usually larger than over land [*Han et*

[1]Institute of Environmental Physics, University of Bremen, Bremen, Germany.
[2]Institute of Physics, National Academy of Sciences of Belarus, Minsk, Belarus.

0148-0227/03/2001JD001543$09.00

al., 1994]. This feature, for instance, is of importance for the simulation of the Earth's climate [*Slingo*, 1989].

[6] A new semianalytical retrieval algorithm for the cloud liquid water path and water droplets size determination has been developed and tested in this study. It is based on the asymptotical solution of the radiative transfer equation for a special case of disperse media with a large optical thickness. This solution was obtained by *Germogenova* [1963] for plane-parallel turbid slabs. Such an approach has already been used in a number of studies [*Rozenberg et al.*, 1978; *King*, 1987]. The difference is that the asymptotical solutions are further simplified such that the inverse problem is reduced to the solution of a single transcendent equation. This allows us to speed up the retrieval process significantly with a minimal loss of accuracy of the retrieved parameters for simulated reflected light fields over optically thick clouds. We do not expect big differences between two models as far as real measurements are concerned.

[7] The algorithm is restricted to the case of optically thick clouds. Thus, we assume that the optical thickness of clouds is larger than approximately 10. For small optical thicknesses, the error increases. Thus, the conventional lookup table approach should be applied in the range of the optical thickness 0–10. In principle, if a high accuracy is not a primary target and one needs to have first order estimates, the algorithm can be also applied down to the optical thickness 5. So in this case the lookup table approach only needs to be applied to optically thin clouds with optical thickness $\tau < 5$. However, it should be stressed that the optical thickness is highly correlated with the geometrical thickness of clouds. For instance, it was shown [*Feigelson*, 1981] that clouds having $\tau < 5$ are characterized by a geometrical thickness less than 200 m. It is difficult to expect that such thin clouds are horizontally homogeneous media. This requires taking the horizontal photon transport into account [*Cahalan et al.*, 1994; *Platnick*, 2001], which is not considered in standard retrieval procedures [*Arking and Childs*, 1985; *Nakajima and King*, 1990]. Due to this inhomogeneity, satellite cloud retrievals for optically thin clouds are troublesome even if the lookup table approach is used. Therefore, we will consider here only that part of our algorithm that is concerned with the case of optically thick clouds.

[8] The paper is organized as follows. In section 2 we review the asymptotic theory of the radiative transfer [*Rozenberg*, 1966; *van de Hulst*, 1980]. We also introduce here the main equation (33), which represents the reflection function of an optically thick weakly absorbing cloud layer over a underlying Lambertian surface with albedo *A*. The auxiliary functions in equation (33) are given in terms of elementary functions (except the reflection function of a semiinfinite nonabsorbing cloud (see, however, equation (5) for a special case of nadir measurements)). As a matter of fact, equation (33) is a very general one and can be used well outside of the framework of this work (e.g., for other weakly absorbing geophysical light scattering media like snow, ice, and foam).

[9] Section 3 is devoted to the application of equation (33) to the semianalytical solution of the cloud inverse problem, namely for finding the effective radius of droplets and cloud liquid water path from a two-channel algorithm. Knowing this, the spectral cloud optical thickness and the number of cloud droplets in a unit column of a cloud volume can be easily obtained as well. Our solution of the inverse problem is a semianalytical one only due to the necessity to solve a simple transcendent equation. This equation is solved using Brent's method [*Brent*, 1973]. In practical terms, it does almost not influence the speed of the retrieval procedure compared to the case of a simple analytical function calculation. This feature could be of importance for operational algorithms, which deal with huge amounts of data. We furthermore study the measurement error propagation in the retrieval scheme (both in numerical and analytical forms) here.

[10] In the conclusions we discuss advantages and disadvantages of the modified asymptotic theory as applied to cloud parameter retrieval. Short appendices present simple analytical approximations for local optical characteristics of clouds like cloud phase function, absorption, and extinction coefficients. A simple and yet accurate parametrization for the cloud asymmetry parameter is also given there. Generally, equations presented in this paper can be used in studies of other problems, well beyond the rather narrow topic of cloud satellite retrievals considered here.

2. The Reflection Function

2.1. The Visible Range

[11] Our main aim in this section is to obtain a simple analytical result for the cloud reflection function in terms of elementary functions, which can be used for the semianalytical satellite cloud retrieval algorithm development. Absorbing and nonabsorbing clouds are considered separately in sections 2.1 and 2.2, respectively. Section 2.3 is devoted to the derivation of new analytical equations for cloud spherical reflectance and total light absorptance in a cloud. Main factors involved in the retrieval procedure are discussed in section 2.4.

[12] To start with, we note that the reflection function of a cloud $R(\vartheta_0, \vartheta, \varphi)$ is defined as the ratio of the reflected light intensity $I(\vartheta_0, \vartheta, \varphi)$ for the case of a cloud to that of an ideal Lambertian white reflector [*Liou*, 1992]:

$$R(\vartheta_0, \vartheta, \varphi) = \frac{I(\vartheta_0, \vartheta, \varphi)}{I^{*(\vartheta_0)}}, \tag{1}$$

where

$$I^*(\vartheta_0) = F \cos \vartheta_0 \tag{2}$$

is the intensity of light reflected from the ideally white Lambertian reflector, πF is the solar flux on the area perpendicular to the direction of incidence, ϑ_0 is the solar angle, ϑ is the observation angle and φ is the relative azimuth between solar and observation directions. We use also: $\mu = |\cos \vartheta|$, $\mu_0 = \cos \vartheta_0$.

[13] It follows for the Lambertian ideally white reflector from equation (1): $R \equiv 1$. This result does not depend on the viewing geometry by definition. Although clouds are white when looking from space, their reflection function $R(\vartheta_0, \vartheta, \varphi)$ is not equal to one. It depends on the viewing geometry. The results of calculations of the reflection function of an idealized semi-infinite nonabsorbing water cloud $R^0_\infty(\vartheta_0, \vartheta, \varphi)$ at the wavelength $\lambda = 650$ nm and the nadir observation are presented in Figure 1. Calculations were performed for the gamma particle size distribution:

$$f(a) = Da^s e^{-s\frac{a}{a_0}}, \tag{3}$$

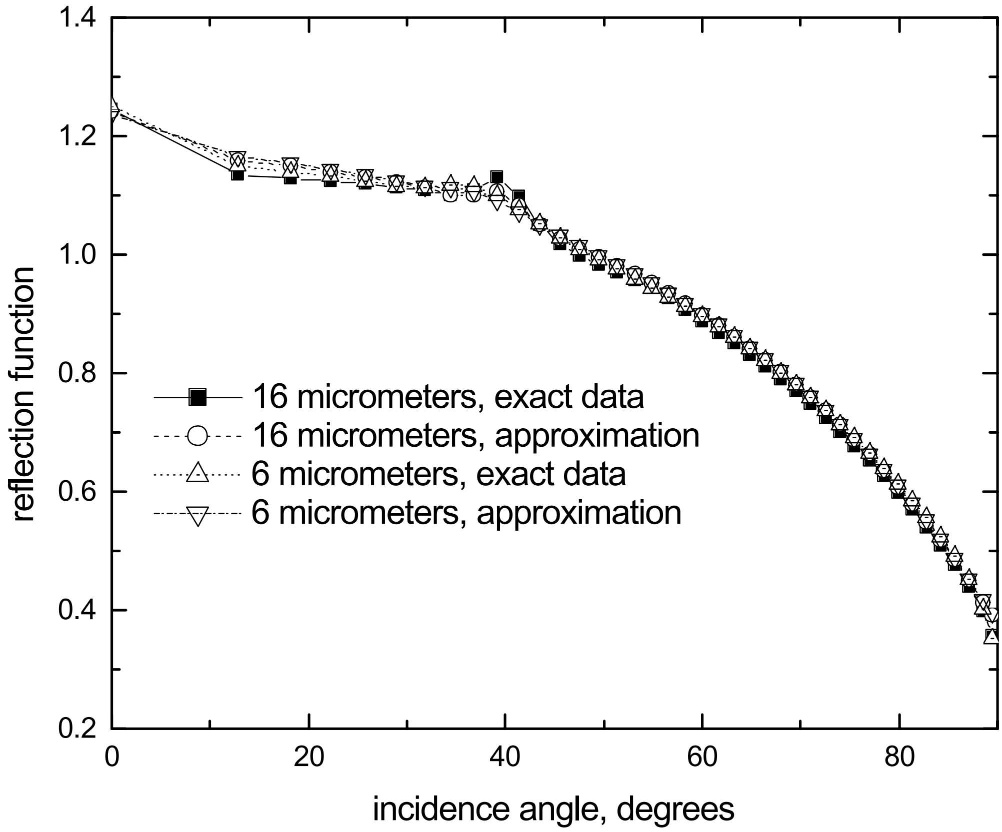

Figure 1. The reflection function of an idealized semiinfinite nonabsorbing cloud $R^0_\infty(0, \vartheta_0, 0)$ at nadir observation obtained from the exact radiative transfer code [*Mishchenko et al.*, 1999] and approximation (5) at wavelength $\lambda = 0.65$ μm and the effective radius of droplets $a_{ef} = 6$ and 16 μm. It is assumed that particles in a cloud are characterized by the gamma particle size distribution.

where $A = \frac{1}{\Gamma(s+1)}\left(\frac{s}{a_0}\right)^{s+1}$ is the normalization constant and a_0 is the mode radius. The half-width parameter s was equal to 6. This value is typical for terrestrial clouds. The effective radius, which is frequently used in cloud remote sensing studies, is defined as a ratio of the third to the second moment of the particle size distribution. In particular, for the distribution given by equation (3) we have:

$$a_{ef} = a_0\left(1 + \frac{3}{s}\right). \tag{4}$$

The values of the effective radius in Figure 1 were 6 and 16 μm. This covers the usual range of variability of the effective radius in natural water clouds. The function $R(\vartheta_0, \vartheta, \varphi)$ can be smaller and larger than 1 depending on the incidence angle. This implies that, for particular viewing geometries, a cloud is even more reflective than the ideally white Lambertian surface. This is mostly due to peculiarities of the phase function of cloudy media (e.g., in the backscattering ($\vartheta \approx \vartheta_0$, $\varphi \approx \pi$) region) for comparatively thick clouds. It follows from Figure 1 that in the range of solar angles 30°–60° and nadir observation the reflection function of a water cloud is almost equal to the reflection function of an ideally white Lambertian reflector. It differs by not more than 10% from 1 for these geometries.

[14] The phase functions $p(\theta)$ (θ is the scattering angle) of water clouds are depicted in Figure A1 (see Appendix A). They are normalized by the following condition: $\frac{1}{2}\int_0^\pi p(\theta)\sin\theta d\theta = 1$. Calculations were performed using the Mie theory at the wavelength of 0.65 μm. The effective radii of water droplets were 4, 6, and 16 μm. The value of s in equation (3) was set to be equal 6. The comparison of Figures 1 and A1 indicates that the phase function is much more sensitive to the effective radius of droplets than the reflection function. We also see that all phase functions of water clouds pass a crossing point around the scattering angle 30°, having a value of approximately 2.27. The phase function is smaller than 1 at scattering angles larger than 43°.

[15] The reflection function $R^0_\infty(\vartheta_0, \vartheta, \varphi)$ can be represented by the following simple approximate equation [*Kokhanovsky*, 2002a]:

$$R^0_\infty(\vartheta_0, \vartheta, \varphi) = \frac{b_1 + b_2\cos\vartheta\cos\vartheta_0 + p(\theta)}{4(\cos\vartheta + \cos\vartheta_0)} \tag{5}$$

where $\theta = \arccos(-\cos\vartheta\cos\vartheta_0 + \sin\vartheta\sin\vartheta_0\cos\varphi)$ is the scattering angle, $p(\theta)$ is the phase function of a cloudy medium (see Appendix A), b_1 and b_2 are constants. Equation (5) obeys to the reciprocity principle [*Zege et al.*, 1991]. It follows for nadir observations [*Kokhanovsky*, 2002a, 2002b]: $b_1 = 1.48$, $b_2 = 7.76$. The results of calculations of the function $R^0_\infty(\vartheta_0, \vartheta, \varphi)$ with equation (5) are presented in Figure 1 along with data, obtained from exact radiative transfer computations. The comparison of

approximate and exact data shows that the accuracy of equation (5) is better than 2% at $\vartheta_0 < 85°$. Constants b_1 and b_2 for other viewing geometries can be found using parametrizations of results obtained from exact radiative transfer codes [e.g., *Mishchenko et al.*, 1999; *Kokhanovsky and Rozanov*, 2003].

[16] Equation (5) can be also used to find the reflection function of a finite cloud $R(\mu, \mu_0, \varphi, \tau)$ by means of the following equation [*Germogenova*, 1963; *van de Hulst*, 1980; *Minin*, 1988; *Kokhanovsky*, 2001]:

$$R(\mu, \mu_0, \varphi, \tau) = R^0_\infty(\mu, \mu_0, \varphi) - t(\tau)K_0(\mu)K_0(\mu_0), \qquad (6)$$

where

$$t = \frac{1}{0.75\tau(1-g)+\alpha} \qquad (7)$$

is the global transmittance of a cloud, $K_0(\mu)$ is the escape function. The escape function is defined via the solution of the characteristic integral equation [*van de Hulst*, 1980]. Note that parameters α and g in equation (7) are defined as follows [*Sobolev*, 1972]:

$$\alpha = 3\int_0^1 K_0(\mu)\mu^2 d\mu, \qquad (8)$$

$$g = \frac{1}{2}\int_0^\pi p(\theta)\sin\theta\cos\theta d\theta. \qquad (9)$$

[17] It should be pointed out that the escape function $K_0(\mu)$ only weakly depends on the cloud microstructure and can be presented by the following simple equation [*Sobolev*, 1972; *Zege et al.*, 1991; *Kokhanovsky*, 2001]:

$$K_0(\mu) = \frac{3}{7}(1+2\mu). \qquad (10)$$

The function $K_0(\mu)$, which was calculated with the exact radiative transfer code for g equal to 0.75, 0.85, and 0.9 in the case of Heney–Greenstein phase function, is presented in Figure 2. We see that $K_0(\mu)$ does almost not depend on g at $\mu \geq 0.2(\vartheta < 78°)$. This is also the case for $g = 0$ and for the Mie-type phase functions. At the range of observation angles $\vartheta = 80°–90°$ there is some dependence of the escape function on the microstructure of the cloud. However, the cloud top nonuniformity plays a role at such grazing observation angles. Therefore the problem cannot be solved in the plane-parallel layer approximation in this case anyway.

[18] The variability of $K_0(\mu)$ at $\mu = 0.2–1.0$ for different values of the average cosine of the scattering angle $g = 0.75–0.9$ is well inside the 2% interval. This coincides with the error of equation (10) at $\mu \geq 0.2$, which is smaller than 2%. This confirms the wide range of applicability of equation (10) in cloud optics. Note that function (10) also describes the angular distribution of the diffused solar light transmitted by a thick cloud. In particular, for the ratio Θ of the diffused transmitted light intensity at the observation angle 60° (from the nadir) to that exactly at the nadir, we have from equation (10): $\Theta = 2/3$, which gives approximately 30% reduction. This can be easily checked experimentally.

[19] The substitution of equation (10) into equation (8) yields:

$$\alpha = \frac{15}{14} \approx 1.07 \qquad (11)$$

independently of the cloud microphysical parameters. It should be pointed out that the value of α, numerically calculated by *King* [1987], assuming the fair weather cumulus cloud model, is approximately 1.07 as well, i.e., in agreement with our estimation. *King* [1987] used the Mie theory to find the phase function of a cloudy medium. *Yanovitskij* [1997] found the same value of α for Heney–Greenstein phase functions with asymmetry parameters in the range 0.0–0.9. This supports the approximation using a fixed value of α in equation (7) given by (11), independently of cloud microphysical parameters.

[20] The accuracy of equation (6) with account for (5), (7), (10), (11), which is used for approximate calculations of the reflection function of a finite cloud in visible, is illustrated in Figures 3a–3c. The error is less than 1% at $\tau \geq 10$ and $\lambda = 0.65$ μm at the nadir observation and a solar angle of 60° (see Figures 3a and 3b). This range of optical thicknesses coincides with the most frequently observed ones in water clouds, both using satellite and ground-based techniques [*Trishchenko et al.*, 2001]. The small, almost constant error at $\tau \geq 30$ is mostly due to the error of approximation (5) for a semi-infinite cloud. Note that errors are negligibly small for all practical purposes for optically thick cloud fields.

[21] The error depends on the solar angle (see Figure 3c). However, it does not exceed 5% at solar angles smaller than 75° for values of $\tau \geq 10$ and $\lambda = 0.65$ μm. The error increases for smaller cloud optical thicknesses (see Figures 3a and 3b). It reaches 4% at $\tau = 5$ for the wavelength 0.65 μm at the nadir observation and solar angle 60° (see Figure 3b). It is highly sensitive to the solar angle at $\vartheta_0 < 40°$ and $\tau = 5$ (see Figure 3c). The detailed study of the accuracy of equation (6) with account for equations (5), (7), (10), and (11) can be found elsewhere [*Kokhanovsky and Rozanov*, 2003]. *Kokhanovsky and Rozanov* [2003] introduced corrections to the asymptotic result (6), which allowed to reduce the error to a level below 5% for all $\tau \geq 5$ for nongrazing solar zenith angles and nadir observation. However, we will not consider this result here and assume the value of $\tau \geq 10$ for this study.

[22] Equation (6) is readily modified to account for the light reflection from an Lambertian underlying surface [*Sobolev*, 1972]:

$$\hat{R}(\mu, \mu_0, \varphi, \tau) = R(\mu, \mu_0, \varphi, \tau) + \frac{AT(\mu)T(\mu_0)}{1-Ar}, \qquad (12)$$

where $\hat{R}$ is the reflection function of a Lambertian surface-cloud system, A is the spherical albedo of an underlying Lambertian surface, which may depend on the wavelength, $R \equiv \hat{R}(A = 0)$,

$$T(\mu) = tK_0(\mu) \qquad (13)$$

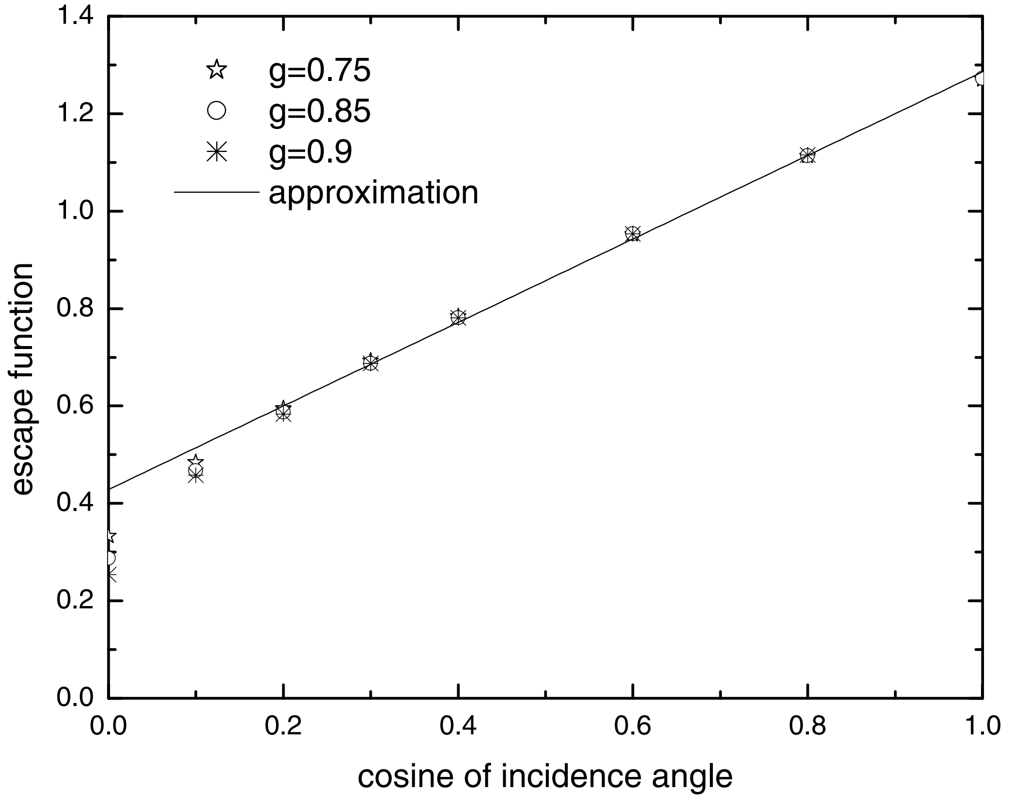

Figure 2. The escape function calculated with exact radiative transfer code for the Heney–Greenstein phase function at $g = 0.75$, 0.8, and 0.9 [*Yanovitskij*, 1997] and with approximation given by equation (10).

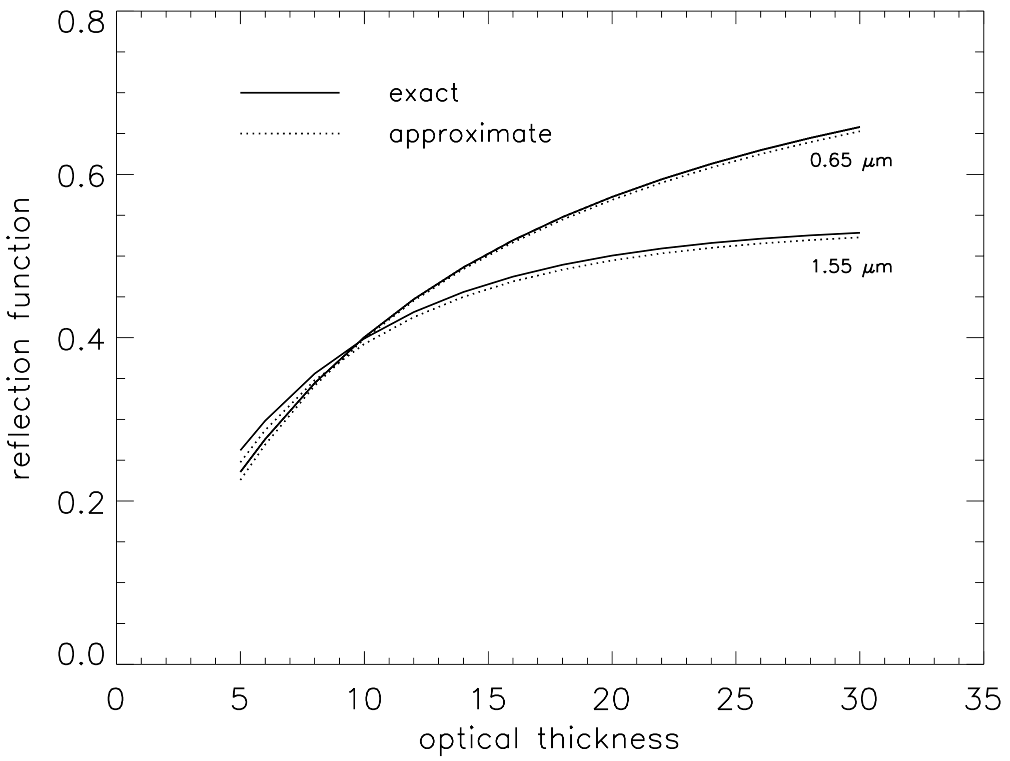

Figure 3a. The dependence of the reflection function of a cloudy layer on the optical thickness according to equations (6) (at $\lambda = 0.65$ μm) and (30) (at $\lambda = 1.55$ μm) at $a_{ef} = 6$ μm, $\vartheta = 0°$, $\vartheta = 60°$ as compared to exact radiative transfer computations.

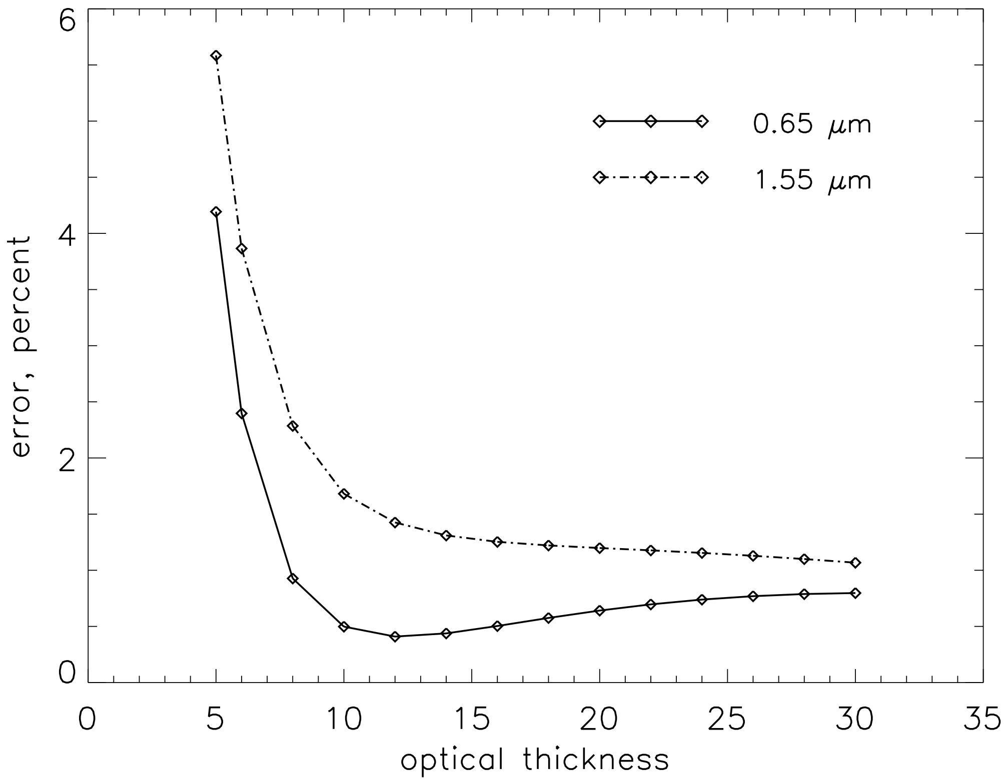

Figure 3b. The errors of approximations given by equations (6) (at $\lambda = 0.65$ μm) and (30) (at $\lambda = 1.55$ μm) at $a_{ef} = 6$ μm, $\vartheta = 0°$, $\vartheta_0 = 60°$ as compared to exact radiative transfer computations.

is the diffuse transmittance of a cloud layer [*Sobolev*, 1972] and r is the spherical albedo of a cloud. Due to the energy conservation law we have: $r = 1 - t$ in visible, where we neglect possible small light absorption inside a cloud. Note that we have neglected the direct solar light term in equation (12). This is possible due to a large thickness of clouds under consideration.

[23] Finally, substituting equations (6) and (13) into equation (12) we have as the reflection function of a

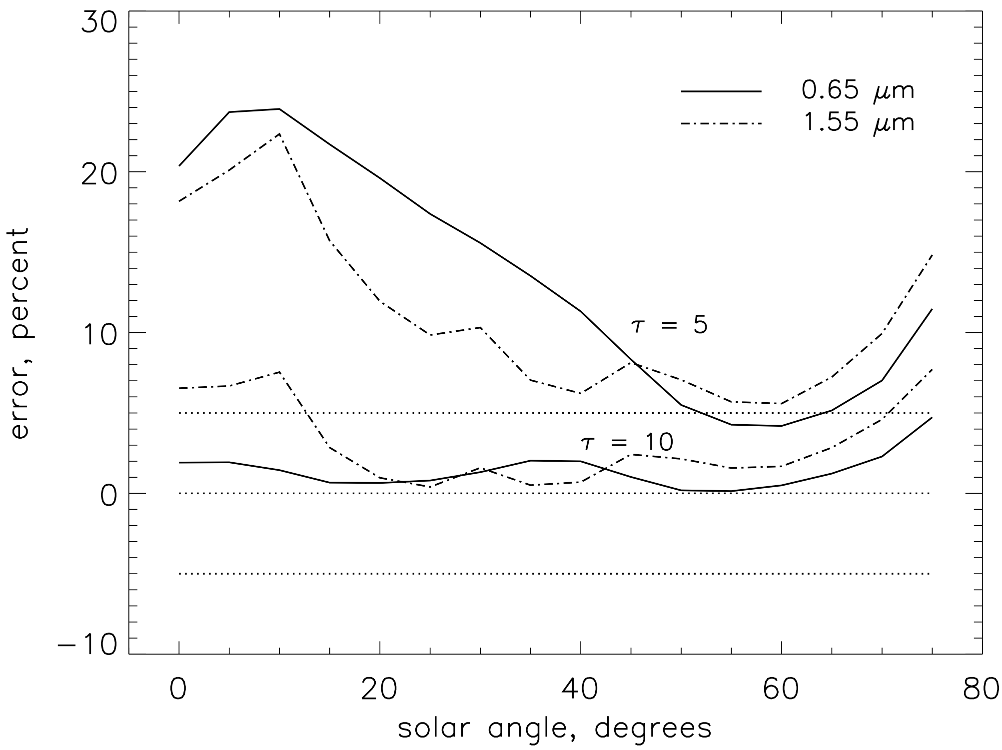

Figure 3c. The same as in Figure 3b, but as the function of the solar zenith angle at $\tau = 5$ and $\tau = 10$.

Lambertian surface-cloud system:

$$\hat{R}(\mu, \mu_0, \varphi, \tau) = R^0_\infty(\mu, \mu_0, \varphi) - \frac{t(1-A)}{1-A(1-t)} K_0(\mu) K_0(\mu_0). \quad (14)$$

This formula with account for equations (5), (7), (10), and (11) will be used as a basis for the semianalytical cloud retrieval algorithm described in section 3.

2.2. The Near-Infrared Range

[24] Unfortunately, the relatively simple equation (6) cannot be applied to the calculation of the reflection function of a finite cloud in the near-infrared region of the electromagnetic spectrum. This is due to the presence of absorption bands of condensed water there. Alternatively, the following formula applies [*Germogenova*, 1963; *van de Hulst*, 1980; *Sobolev*, 1984; *King*, 1987]:

$$R(\mu, \mu_0, \varphi, \tau) = R_\infty(\mu, \mu_0, \varphi) - \frac{mle^{-2\gamma\tau}}{1 - l^2 e^{-2\gamma\tau}} K(\mu) K(\mu_0), \quad (15)$$

where γ is the diffusion exponent, $K(\mu)$ and R_∞ are the escape function and the reflection function of an absorbing semiinfinite medium with the same local optical characteristics as a finite layer under study, respectively. Equation (15) accounts for the influence of light absorption on the reflection function of clouds. Clearly, the reflection function decreases if additional absorbers are present in cloud droplets for the same phase function. Such a decrease is characteristic for the infrared channels, where water itself is a relatively strong absorber of solar radiation.

[25] Constants l and m are defined by the following integrals [*van de Hulst*, 1980]:

$$l = 2 \int_0^1 K(\mu) i(-\mu) \mu d\mu, \quad (16)$$

$$m = 2 \int_{-1}^1 i^2(\mu) \mu d\mu, \quad (17)$$

$i(\eta)$ being the angular distribution of light in deep layers of a cloud, where the so-called asymptotic regime takes place [*Sobolev*, 1972]. Functions $i(\mu)$, $K(\mu)$, $R^0_\infty(\mu, \mu_0, \varphi)$ can be found from the solution of correspondent integral equations [*Sobolev*, 1972; *van de Hulst*, 1980].

[26] Functions $R_\infty(\mu, \mu_0, \varphi)$, $K(\mu)$ and constants m and l have the following asymptotic forms when light absorption by droplets is relatively small (single-scattering albedo $\omega_0 \to 1$) [*van de Hulst*, 1980; *Minin*, 1988]:

$$R_\infty(\mu, \mu_0, \varphi) = R^0_\infty(\mu, \mu_0, \varphi) - 4\sqrt{\frac{1-\omega_0}{3(1-g)}} K_0(\mu) K_0(\mu_0), \quad (18)$$

$$K(\mu) = K_0(\mu)\left(1 - 2\alpha\sqrt{\frac{1-\omega_0}{3(1-g)}}\right), \quad (19)$$

$$m = 8\sqrt{\frac{1-\omega_0}{3(1-g)}}, \quad (20)$$

$$l = 1 - 4\alpha\sqrt{\frac{1-\omega_0}{3(1-g)}}, \quad (21)$$

and $\gamma \to \sqrt{3(1-\omega_0)(1-g)}$ as the single scattering albedo $\omega_0 \to 1$. Note that we have at $\omega_0 = 1$: $R_\infty \equiv R^0_\infty$, $K(\mu) \equiv K_0(\mu)$, $m = 0$, $l = 1$. Taking correspondent limits, we obtain that equation (15) transforms into equation (6) in this case as it should be. Interestingly, as it follows from the asymptotic analysis [*van de Hulst*, 1980], the absorption reduces the cloud reflection function equally for all relative azimuths as $\omega_0 \to 1$ (see equation (18)).

[27] We underline that equations (18)–(21) follow from the asymptotic analysis of the radiative transfer equation. The integration of equation (18) with respect to all angles yields [*Kokhanovsky*, 2001]: $r_\infty = 1 - y$, where $y = 4\sqrt{\frac{1-\omega_0}{3(1-g)}}$ and r_∞ is the spherical albedo of a weakly absorbing semi-infinite cloud [*van de Hulst*, 1980]. This result is valid only as $y \to 0$. Thus, the parameter y (as $\omega_0 \to 1$) can be interpreted as a fraction of photons, absorbed in a weakly absorbing semi-infinite cloud for a diffuse illumination. It depends both on the single scattering albedo and the asymmetry parameter. Clouds having larger values of g, therefore, absorb more light. Larger values of g imply that photon scattering increases at small angles. Thus the photon path length before its escape from the medium is also increased. As a consequence, this results in increased light absorption in the medium. Media having different values of ω_0 and g, but the same values of y, have the same values of r_∞ under the approximation considered here. The parameter y (divided by four and with $g\omega_0$ substituted by g) is called the similarity parameter [*van de Hulst*, 1980]. It is a useful parameter, describing the optical properties of clouds. Substituting y into equations (18)–(21) yields:

$$R_\infty(\mu, \mu_0, \varphi) = R^0_\infty(\mu, \mu_0, \varphi) - yK_0(\mu) K_0(\mu_0), \quad (22)$$

$$K(\mu) = K_0(\mu)\left(1 - \frac{\alpha y}{2}\right), \quad (23)$$

$$m = 2y, \quad (24)$$

and

$$l = 1 - \alpha y. \quad (25)$$

Equations (22)–(25) were derived assuming that $\omega_0 \to 1$. Alternatively, the right-hand sides of equations (22)–(25) give us the first terms of the expansion of correspondent functions with respect to y. The accuracy of equations decreases with the probability of photon absorption $\beta = 1 - \omega_0$. The higher terms of the expansions (22)–(25) are not known or quite complex [*Minin*, 1988]. However, it has been shown that the following equations (see also equation (15)) approximately account for higher order terms [*Rozenberg*, 1962; *Zege et al.*, 1991; *Kokhanovsky et al.*, 1998]:

$$R_\infty(\mu, \mu_0, \varphi) = R^0_\infty \exp(-yu(\mu, \mu_0, \varphi)), \quad (26)$$

$$mK(\mu)K(\mu_0) = \left(1 - e^{-2y}\right) K_0(\mu) K_0(\mu_0), \quad (27)$$

$$l = \exp(-\alpha y), \tag{28}$$

where a viewing function is defined by

$$u(\mu, \mu_0, \varphi) = \frac{K_0(\mu)K_0(\mu_0)}{R^0_\infty(\mu, \mu_0, \varphi)} \tag{29}$$

and does not depend on ω_0 and τ by definition. The viewing function only has a weak dependence on the microphysical parameters of clouds (e. g., the droplet size distribution). This fact follows from the low sensitivity of the functions $R^0_\infty(\mu, \mu_0, \varphi)$, $K_0(\mu)$ in equation (29) to the microstructure of clouds (see Figures 1 and 2).

[28] It should be stressed that the approximations (26)–(28), (5), (10), and (11) allow to avoid the solution of integral equations [*van de Hulst*, 1980; *Yanovitskij*, 1997] for the determination of functions $R_\infty(\mu, \mu_0, \varphi)$ and $K(\mu)$ in equation (15). This is of a general importance. Note, that equations (26) and (28) transform to exact asymptotic results (22) and (25) as $y \to 0$.

[29] Substituting equations (27) and (28) into equation (15), we have:

$$R(\mu, \mu_0, \varphi, \tau) = R_\infty(\mu, \mu_0, \varphi) - te^{-x-y}K_0(\mu)K_0(\mu_0), \tag{30}$$

where $x = \gamma\tau$. Note that the value of $\exp(-x)$ describes the attenuation of light field in deep layers of a cloud [*van de Hulst*, 1980].

[30] It can be easily shown [*Kokhanovsky*, 2001] that the parameter t in equation (30) gives the global transmittance for a nonabsorbing cloud field:

$$t = \frac{\sinh y}{\sinh(\alpha y + x)} \tag{31}$$

Importantly, equation (31) yields equation (7) at $\omega_0 = 1$.

[31] Equation (30) was first proposed by *Rozenberg* [1962]. However, his derivation differs from that presented here. Also he proposed equation (31) with $\alpha = 1$, which is not consistent with the exact asymptotic result, given by equation (7).

[32] The range of applicability of equation (26) with respect to higher values of y can be readily extended using the following simple correction:

$$R_\infty(\mu, \mu_0, \varphi) = R^0_\infty(\mu, \mu_0, \varphi)\exp(-y(1 - cy)u(\mu, \mu_0, \varphi)). \tag{32}$$

where $c = 0.05$ [*Kokhanovsky*, 2002b]. The value of c was obtained by the parametrization of exact radiative transfer calculations [*Mishchenko et al.*, 1999].

[33] The accuracy of equations (30)–(32) with account for equations (5), (10), and (11) for the wavelength $\lambda = 1.55$ µm, where water only weakly absorbs radiation, was investigated. Selected results are presented in Figures 3a–3c. It was assumed that the effective radius of droplets is equal to 6 µm and the parameter $s = 6$ in equation (3). The Mie calculations for this case yield: $\omega_0 = 0.9935$, $g = 0.8214$. It follows from Figures 3a and 3b that equation (30) is an accurate representation for $\tau \geq 10$, $\vartheta = 0°$, $\vartheta_0 = 60°$. The error is less than 2% for this case, which is a relatively small error, compared to the uncertainty in forward cloud models applied to the real atmosphere (e. g., vertically and horizontally inhomogeneous cloud fields). The constant error at $\tau > 30$ is mostly due to the error of the approximation for the reflection function of a semi-infinite cloud, given by equation (32). The error increases with the optical thickness and reaches 5.5% at $\tau = 5$ (see Figures 3a and 3b) in the case under study.

[34] The error depends on the solar zenith angle. This is shown in Figure 3c. It is smaller than 5% for solar zenith angles, ranging from 12° to 75° at $\tau = 10$ and nadir observation. The error reaches 22% for the optical thickness $\tau = 5$ and the solar zenith angle 10°. It is, however, around 5% at the solar angle of 60° for the same optical thickness (see Figure 3c). Thus, equations (30)–(32) can be applied to clouds with $\tau < 10$ with a great care. In particular, the solar angle should be in the range 50°–65° to have an accuracy lower than 7% at $\tau = 5$. More complete studies of accuracy are given by *Kokhanovsky and Rozanov* [2003]. They also introduced a correction term in equation (30), which allowed to reduce errors of equation (30) well below 5% at $\tau = 5$ for all solar angles smaller 75°. However, we will not use the modified solution given by *Kokhanovsky and Rozanov* [2003] here and consider clouds with $\tau \geq 10$. This allows to simplify the cloud retrieval algorithm presented here. The modified solution, given by *Kokhanovsky and Rozanov* [2003], can be easily incorporated in the cloud retrieval scheme, if clouds in the range of the optical thickness 5–10 are of interest.

[35] The comparison of data for wavelengths 0.65 and 1.55 µm, presented in Figure 3a, show us that the limit of the semi-infinite cloud is reached more rapidly for infrared absorbing wavelengths, where water is a more absorbing substance than in the visible. As it will be shown in the next section, this result can be used in the estimation of the droplets size even if the optical thickness of clouds itself is not retrieved.

[36] Interestingly, both curves in Figure 3a cross around the optical thickness 10. At optical thicknesses lower than 10, the reflection function at the absorbing channel is higher. This is because of the differences in the phase function between the visible and infrared spectral regions.

[37] Equation (30), which includes equation (6) as a special case, can be used to determine the optical thickness and effective radius from spectral reflection function measurements over extended cloud fields.

[38] The Lambertian surface reflection is accounted for by equation (12). The substitution of equation (30) into equation (12) yields:

$$\hat{R}(\mu, \mu_0, \varphi) = R_\infty(\mu, \mu_0, \varphi) - \left[\exp(-x - y) - \frac{At}{1 - Ar}\right]T(\mu, \mu_0), \tag{33}$$

where

$$\mathrm{T}(\mu, \mu_0) = tK_0(\mu)K_0(\mu_0) \tag{34}$$

is the transmission function of a cloud, r is the total reflectance of the cloud or the spherical albedo. The values of t and R_∞ are given by equations (31) and (32)

respectively. Strictly speaking, equation (33) is only valid for channels, where the single scattering albedo ω_0 is close to one. Note that for typical values of the cloud droplet effective radii 4–16 μm the value of $\omega_0 = 0.985–0.996$ for the wavelength 1.55 μm, which is indeed close to one. For the wavelengths 1.64 and 2.15 μm, which are often used in cloud retrievals, the values of ω_0 lay in the range 0.991–0.998 and 0.970–0.993 respectively for the same interval of the cloud effective radius change. Overall, the probability of photon absorption $\beta = 1 - \omega_0$ is smaller than 0.035 for wavelengths $\lambda \leq 2.3$ μm and $a_{ef} \leq 16$ μm. In this case the parameter $y < 1.1$.

[39] Equation (33) is a key formula for this study. Its accuracy (also with account for correction terms) is studied in detail elsewhere [*Kokhanovsky and Rozanov*, 2003].

[40] Note that equation (33) can be easily generalized to account for the bidirectional surface reflectance effects. We will not discuss this matter in any detail here, however.

2.3. The Total Reflectance

[41] The only parameter in equation (33), which is not represented by simple functions, is the total reflectance r. Let us find now the approximate solution for the value of r in equation (33) in terms of elementary functions. Clearly, the value of $r \neq 1 - t$ due to light absorption effects.

[42] To start with, we remind that the total reflectance or the spherical albedo r is defined by the following equation [*Sobolev*, 1972]:

$$r = \int_0^{\pi/2} d\vartheta_0 \sin 2\vartheta_0 \Re(\vartheta_0),$$
$$\Re(\vartheta_0) = \frac{1}{2\pi}\int_0^{2\pi} d\varphi \int_0^{\pi/2} d\vartheta \sin 2\vartheta R(\vartheta_0, \vartheta, \varphi) \tag{35}$$

Here, $\Re(\vartheta_0)$ is the plane albedo [*Sobolev*, 1972]. For the case of idealized semiinfinite nonabsorbing clouds [*Sobolev*, 1972] and as a result of the conservation of energy law, we have:

$$\frac{1}{2\pi}\int_0^{2\pi} d\varphi \int_0^{\pi/2} d\vartheta_0 \sin 2\vartheta_0 \int_0^{\pi/2} d\vartheta \sin 2\vartheta R^0_\infty(\vartheta_0, \vartheta, \varphi) = 1 \tag{36}$$

and also

$$\frac{1}{2\pi}\int_0^{2\pi} d\varphi \int_0^{\pi/2} d\vartheta \sin 2\vartheta R^0_\infty(\vartheta_0, \vartheta, \varphi) = 1, \tag{37}$$

i.e., all photons injected into a cloudy medium are reflected back into outer space after an infinite travel time. Here, $R^0_\infty(\vartheta_0, \vartheta, \varphi)$ is the reflection function of a semi-infinite nonabsorbing cloud. The reflection function $R^0_\infty(\vartheta_0, \vartheta, \varphi)$ of a cloudy medium only weakly depends on its microstructure (see Figure 1) and (by definition) it does not depend on either the optical thickness $\tau = \sigma_{ext}L$ or the single scattering albedo $\omega_0 = \sigma_{sca}/\sigma_{ext}$. Here σ_{ext} is the extinction coefficient and σ_{sca} is the scattering coefficient of a cloudy layer of the geometrical thickness L.

[43] It follows from equations (30) and (35) for light absorbing clouds:

$$r = r_\infty - t\exp(-x - y), \tag{38}$$

where

$$r_\infty = \int_0^{\pi/2} d\vartheta_0 \sin 2\vartheta_0 \Re(\vartheta_0),$$
$$\Re_\infty(\vartheta_0) = \frac{1}{2\pi}\int_0^{2\pi} d\varphi \int_0^{\pi/2} d\vartheta \sin 2\vartheta R_\infty(\vartheta_0, \vartheta, \varphi). \tag{39}$$

The normalization condition [*van de Hulst*, 1980]

$$2\int_0^1 d\mu\mu\, K_0(\mu) = 1 \tag{40}$$

was used to derive equation (38). Note that approximation (10) is consistent with equation (40). Now, we need to find the expression for the value of r_∞, given by equation (39). The constant r_∞ represents the total reflectance of a semi-infinite layer. According to the definition (36), $r_\infty = 1$ at $\omega_0 = 1$. Equation (39) is not readily analytically integrated at arbitrary values of ω_0, however. So we make the approximate integration in equation (39). First of all, we note that it follows from equation (39) as $\omega_0 \to 1$ (see also the discussion in the previous section):

$$r_\infty = 1 - y. \tag{41}$$

To derive equation (41) we have used formulae (18), (36), and (40). At larger values of y, we will use the same substitution as was used in the derivation of equation (28) from equation (25). Then we have for the integral (39):

$$r_\infty = \exp(-y) \tag{42}$$

or (see equation (28)): $r_\infty = l^{1/\alpha}$. Note that it follows: $\alpha \approx 1$ and $l \approx r_\infty$. This is an interesting result by itself. The accuracy of equation (42) was studied in detail by *Kokhanovsky* [2002b]. It can be applied at least up to $y \approx 1$.

[44] Combining equations (31), (38), and (42), we have for the total reflectance of a cloud layer:

$$r = \frac{\sinh(x + \alpha y)\exp(-y) - \sinh(y)\exp(-x - y)}{\sinh(x + \alpha y)}. \tag{43}$$

The substitution of equation (43) into equation (33) enables us to obtain the reflection function of a cloud-underlying surface system in terms of the elementary functions, assuming that the reflection function of a semi-infinite nonabsorbing cloud is known (see equations (32) and (5)). This is the major result of this work.

[45] Having r and t, one can also find the plane albedo [*Zege et al.*, 1991; *Kokhanovsky*, 2001] $\Re(\mu_0) = \Re_\infty(\mu_0) - T(\mu_0)\exp(-x - y)$, the diffuse transmission $T(\mu_0) = tK(\mu_0)$ and the absorptance $A(\mu_0) = 1 - \Re(\mu_0) - T(\mu_0)$. The diffuse

transmission is defined by an equation similar to equation (35) for a plane albedo, but with the transmission (34) and not the reflection function (33) as an integrand. Note that $\Re_\infty(\mu_0) = \exp(-yK_0(\mu_0))$ is the plane albedo of a semi-infinite layer [*Zege et al.*, 1991; *Kokhanovsky*, 2001]. Functions $\Re(\mu_0)$ and $T(\mu_0)$ are often measured experimentally (see results presented by *Los and Duynkerke* [2000]). For visible channels, where light absorption can be neglected, we have: $\Re(\mu_0) = 1 - T(\mu_0)$. Functions $K_0(\mu_0)$ and $T(\mu_0)$ decrease with the solar angle. This means that the plane albedo increases with the solar angle, which is opposite to the dependence of the reflection function at a nadir observation, given in Figure 1. Smaller values of the plane albedo for higher Sun positions were also observed experimentally [*Los and Duynkerke*, 2000].

[46] The total light absorptance in a cloud layer is given by: $a = 1 - r - t$, where r is calculated by equation (43) and t by equation (31). As a result, we have the following analytical equation for the total light absorption inside a plane-parallel cloud with a finite optical thickness:

$$a = \frac{\sinh(x+\alpha y)(1-\exp(-y)) - \sinh(y)(1-\exp(-x-y))}{\sinh(x+\alpha y)}, \tag{44}$$

where the diffuse illumination of a cloud layer is assumed. It follows as $\alpha \equiv 1$ from equations (31), (43), (44):

$$r = \frac{\sinh(x)}{\sinh(x+y)},\quad t = \frac{\sinh(y)}{\sinh(x+y)},\quad a = \frac{\sinh(x+y) - \sinh(x) - \sinh(y)}{\sinh(x+y)}, \tag{45}$$

which yields the well-known formulae, presented elsewhere [e.g., *Zege et al.*, 1991].

2.4. Similarity Parameters

[47] We see that the global radiative characteristics of cloudy media are well described by only two parameters: $x = \tau\sqrt{3(1-\omega_0)(1-g)}$ and $y = 4\sqrt{\frac{1-\omega_0}{3(1-g)}}$. We will call them similarity parameters. Let us discuss their relationships with microphysical properties of clouds, in particular with the sizes of droplets and their complex refractive index.

[48] The physical sense of the parameter y was discussed above. It is equal to the logarithm of the inverse value of the spherical albedo of a semiinfinite weakly absorbing light scattering cloud layer (see equation (42)). The parameter x describes the attenuation of a light field in deep layers of semi-infinite weakly absorbing media. Namely, we have for the light intensity in deep layers: $I(\mu, \tau) \sim i(\mu)\exp(-x)$, where the angular distribution of light field $i(\mu)$ does not depend on the optical depth τ. Thus, we see that radiative characteristics of optically thick layers are determined by parameters, which govern light reflection and asymptotic regime for semiinfinite media. This is an important result of the radiative transfer theory, which has not yet been fully exploited for the solution of remote sensing problems.

[49] The transformation of x and y yields another set of parameters: $p \equiv xy$ and $q \equiv x/y$, where $p = 4\tau_{abs}$, $q = \frac{3}{4}\tau^*$. Here $\tau_{abs} \equiv \sigma_{abs}L$ is the optical thickness resulting from light absorption and $\tau^* = \sigma_{ext}(1-g)L$ is the scaled optical thickness, which is smaller than the cloud optical thickness by a factor $(1-g)$. The following parameters such as the absorption length $L_{abs} = 1/\sigma_{abs}$ and the reduced extinction length $L^*_{ext} = 1/[\sigma_{ext}(1-g)]$ can also be introduced. Therefore, we see that values of r, t, and a for optically thick weakly absorbing media only depend on the ratios L/L_{abs}, L/L^*_{ext}. The details of the angular distribution of light in a single scattering event are of a secondary importance for this assumed case.

[50] Let us estimate the dependence of parameters p and q on the effective radius a_{ef} of droplets. For this we will assume that droplets are large ($ka_{ef} \to \infty$) and weakly absorbing ($\kappa a_{ef} \to 0$), which is appropriate for water droplets in the visible and near-infrared regions of the electromagnetic spectrum. Here $k = 2\pi/\lambda$ is the wave number and $\kappa = 4\pi\chi/\lambda$ is the absorption coefficient of water (χ is the imaginary part of the refractive index of droplets and λ is the wavelength of the incident light). To the first coarse approximation (see Appendix B), extinction and absorption coefficients are given by:

$$\sigma_{ext} = \frac{1.5C_v}{a_{ef}},\quad \sigma_{abs} = 1.25\kappa C_v,\ 1-g = 0.12 \tag{46}$$

where C_v is the volumetric concentration of droplets. The value of C_v is the fraction of a unit volume occupied by droplets in a cloud. It is a small figure. For example, assuming that $C_v \approx 10^{-7}$ we obtain: $\sigma_{ext} \approx 0.025^{-1}$ at $a_{ef} \approx 6$ μm, which is inside the variability range for the value of σ_{ext} in natural clouds [*Zege et al.*, 1991; *Los and Duynkerke*, 2000].

[51] The probability of photon absorption $\beta = \sigma_{abs}/\sigma_{ext}$ can also be obtained from equation (46): $\beta = \frac{5}{6}\kappa a_{ef}$. For p and q we have to a first approximation, therefore:

$$p = 5\kappa w/\rho,\quad q = 0.14w/\rho a_{ef}, \tag{47}$$

Here $w = C_v L\rho$ is the liquid water path and $\rho = 1000$ kg/m^3 is the density of water.

[52] This means that the parameter p does not depend on the size of droplets at all in the framework of the approximation considered. The value of p is determined only by the product of the absorption coefficient of water and the liquid water path of a cloud. The parameter q, on the other hand, does not depend on the refractive index of droplets. It is determined by the ratio of the liquid water path $w = C_v L\rho$ to the effective size of droplets a_{ef}. This means that both the imaginary part of the refractive index of droplets x and the values a_{ef}, w can be in principle determined from the measurements of the backscattered radiation from clouds.

[53] In the next section it will be assumed that the spectral dependence $\kappa(\lambda)$ is known. This assumption allows us to find the effective radius of droplets and the liquid water path of cloudy media from satellite measurements of the reflection functions of clouds. Note, however, that the uncertainty related to imperfect knowledge of the temperature-dependent absorption coefficient $\kappa(\lambda)$ for real cloud systems could be quite large [*Asano et al.*, 2000].

[54] Using relationships between (x, y) and (p, q) one obtains approximately:

$$x = \frac{4w}{5\rho}\sqrt{\frac{\kappa}{a_{ef}}},\quad y = 6\sqrt{\kappa a_{ef}}, \tag{48}$$

where the value of y is determined by the effective size of droplets and $x \sim w/\sqrt{a_{ef}}$. Although the dependencies presented in equation (48) are only approximations of a real situation in cloudy media, they illustrate the origin of the parameters used to describe the local optical characteristics of clouds quite well. It should be pointed out that the reduced optical thickness $\tau^* = \tau(1 - g)$ (see equation (7)) is given by the ratio $4x/3y$ or $\tau^* \approx 8w/45\rho a_{ef}$.

3. The Inverse Problem

3.1. The Cloud Optical Thickness Determination

[55] Now all equations are prepared to proceed to the solution of the inverse problem. In particular, parameters a_{ef} and w can be found as roots of following functions:

$$F_i(a_{ef}, w) = \hat{R}_i(\mu, \mu_0, \varphi) - R_{\infty i}(\mu, \mu_0, \varphi) + \frac{t_i e^{-x_i - y_i} - A_i t_i (t_i + r_i e^{-x_i - y_i})}{1 - A_i r_i} K_0(\mu_0) K_0(\mu), \quad (49)$$

where $i = 1, 2, 3, \ldots N$ corresponds to a given measurement channel and $\hat{R}_i$ is the measured reflected function at that channel. N is the total number of channels used in a retrieval procedure. For reasons of simplicity and clarity, we assume that all possible atmospheric influences (like gaseous and aerosol absorption and scattering) are subtracted from measured reflection functions and $\hat{R}_i$ is the so-called refined reflection function. For the same reason, we avoid the integration of equation (49) with respect to the spectral response function of the instrument and the spectral change in the solar constant for a given instrument response function.

[56] In this paper we will only consider one-channel ($N = 1$) and two-channel ($N = 2$) algorithms. The generalization to the case of an arbitrary number of channels is trivial. The two-channel algorithm constitutes a minimum set of experimental values to determine two unknown parameters (a_{ef} and w) as simultaneous roots of functions $F_1(a_{ef}, w)$ and $F_2(a_{ef}, w)$. This does not mean, however, that the one-channel algorithm does not provide us with any useful information. To be more explicit, let us suppose that the wavelength, of which the measurement is performed, belongs to the visible range of the electromagnetic spectrum. In this case we have with a high accuracy (see equation (47)): $p = 0$ and we are left with the necessity of finding only one parameter $q = x/y$, which is the root of the function $F_1(q)$. Then the value of $\tau^* = \frac{4}{3}q$ can be easily found.

[57] The discussion of the two-channel algorithm will be postponed to the next subsection. Let us consider the one-channel algorithm (at $\omega_0 = 1$) in more detail. For this we need to return to equation (14), which gives:

$$t = \frac{(1 - A)\Lambda}{1 - A(1 + \Lambda)}, \quad (50)$$

where the function Λ is introduced and given by

$$\Lambda \equiv \Lambda(\mu, \mu_0, \varphi) = \frac{R^0_\infty(\mu, \mu_0, \varphi) - \hat{R}(\mu, \mu_0, \varphi, \tau)}{K_0(\mu) K_0(\mu_0)}. \quad (51)$$

The analytical results for functions $R^0_\infty(\mu, \mu_0, \varphi)$ and $K_0(\mu)$ have been presented above (see equations (5) and (10) and Appendix A). Thus, the global transmittance t, and, correspondingly, the total reflectance $r = 1 - t$ of extended cloud fields can be obtained from equations (50) and (51), and a knowledge of the surface albedo A, angles ϑ_0, ϑ, φ and the measured value $\hat{R}(\mu, \mu_0, \varphi, \tau)$. For such a retrieval, one does not need to know the optical thickness of clouds and the average size of droplets. This is of significance for climate studies, where the globally and temporally averaged value of the cloud reflectance r is an important parameter. Note that for measurements over oceans (and over land for sufficiently small values of λ (e.g., 400 nm)), the value of A is small and can be neglected in a first coarse approximation.

[58] Let us consider equation (50) in more detail now. First of all, we have at $A = 0$: $t \equiv \Lambda$ and, second, $t = 0$ and $r = 1$ at $A = 1$. This shows that all photons entering optically thick clouds over surfaces with $A = 1$ survive and return back to outer space. They yield no information about actual cloud thickness. This explains why the retrieval of cloud parameters over bright surfaces (e.g., snow and ice) cannot be performed in visible. This issue, however, will be discussed in the next section in more detail.

[59] The information on the global transmittance t can be used to find the scaled optical thickness $\tau^* = \tau(1 - g)$. It follows from equation (7):

$$\tau^* = \frac{4}{3}\left[t^{-1} - \alpha\right], \quad (52)$$

where t is given by equation (50). Again the value of τ^* can be obtained without knowledge of the size of droplets and the actual optical thickness of clouds.

[60] Equation (52) can be used for the retrieval of τ^* from the measurement $\hat{R}(\mu, \mu_0, \varphi, \tau)$ at a single wavelength. The functions $R^0_\infty(\mu, \mu_0, \varphi)$ and $K_0(\mu_0)$ in equation (51) and the parameter α in equation (52) are defined by equations (5), (10), and (11), respectively.

[61] One can apply equation (50) for the derivation of the optical thickness τ as well if the value of g is known. However, the asymmetry parameter g only slightly depends on the size of droplets for nonabsorbing channels [*Kokhanovsky*, 2001]:

$$g = g_0 - \frac{\Upsilon}{(ka_{ef})^{2/3}}, \quad (53)$$

where $g_0 \approx 0.884$, $\Upsilon \approx 0.5$, $k = \frac{2\pi}{\lambda}$. Often, the dependence $g(a_{ef})$ is neglected and it is assumed that $a_{ef} = 10$ μm [*Rossow and Schiffer*, 1999]. In this case it follows from equation (53): $g = 0.86$ at $\lambda = 0.65$ μm and $a_{ef} = 10$ μm. This value of g can be used for a crude estimation of the optical thickness from the value of τ^*.

[62] Clearly, errors can be introduced, if one assumes the fixed a priori defined value of g. Indeed the value of a_{ef} is usually in the range 4–20 μm [*Han et al.*, 1994]. Then it follows from equation (53) at $\lambda = 0.65$ μm that $g = 0.84$–0.87 at $a_{ef} = 4$–20 μm. Also we have: $\tau = \upsilon\tau^*$, where $\upsilon \equiv (1 - g)^{-1} \approx 6.3$–$7.6$ and $\tau \in [9.4, 11.5]$ at $\tau^* = 1.5$, depending on the value of g used. The assumption that $a_{ef} = 10$ μm yields: $g = 0.86$ and $\upsilon = 7.2$, $\tau = 10.7$. This leads to a relative error of 7–14% in the retrieved optical thickness, depending on the actual value of a_{ef}. This uncertainty in the optical thickness determination can be removed if measurements in the near-infrared region of the electromagnetic spectrum are performed, enabling the size of droplets and, therefore, the parameter g (see equation (53)) to be estimated.

3.2. The Two-Channel Inversion Algorithm

[63] As it was specified above for the correct estimation of the optical thickness of clouds from space we need to know the effective radius of droplets. The size of droplets can be found if the reflection function in the near-infrared region of the electromagnetic spectrum is measured simultaneously with measurements in the visible range. This is due to the fact that the reflection function in the infrared strongly depends on the probability β of photon absorption by local volume of a cloud medium. This probability is proportional to the effective radius of droplets, as it was discussed above ($\beta \approx \kappa a_{ef}$) (see section 2.4).

[64] The influence of absorption and scattering of light by molecules and aerosol particles on the measured value $R(\mu, \mu_0, \varphi, \tau)$ is neglected in the retrieval algorithm presented here. However, corrections can be easily taken into account if needed [*Bucholtz*, 1995; *Wang and King*, 1997; *Goloub et al.*, 2000]. The influence of the surface reflection on the cloud reflection function, assuming that the surface is Lambertian with albedo *A,* is taken into account. Then it results (see equations (14) and (33)):

$$\hat{R}_1(a_{ef}, w) = R_\infty^0 - \frac{t_1(a_{ef}, w)[1 - A_1]}{1 - A_1[1 - t_1(a_{ef}, w)]} K_0(\mu) K_0(\mu_0), \quad (54)$$

$$\begin{aligned} \hat{R}_2(a_{ef}, w) = {} & R_\infty^0 \exp(-y(a_{ef})(1 - cy(a_{ef}))u) \\ & - \left[\exp(-x(a_{ef}, w) - y(a_{ef})) - \frac{t_2(a_{ef}, w) A_2}{1 - A_2 r_2(a_{ef}, w)}\right] \\ & \cdot t_2(a_{ef}, w) K_0(\mu) K_0(\mu_0). \end{aligned} \quad (55)$$

[65] The subscripts "1" and "2" refer to wavelengths λ_1 and λ_2 in visible and near-infrared channels, respectively. The values of A_1 and A_2 give us the surface albedos in visible and near infrared, respectively. We assume that both A_1 and A_2 are known. $\hat{R}_1$ and $\hat{R}_2$ are measured reflected functions at the visible and near-infrared channels, respectively. Any weak spectral dependence of the function $R_\infty^0(\lambda)$ due to the third term in the nominator of equation (5) is considered negligible because of small values of this term for most geometries. The explicit dependence of functions involved on the parameters a_{ef} and w we are going to retrieve is introduced in brackets. The liquid water path w is preferred to the optical thickness in the retrieval procedure due to the independence of w of the wavelength. The optical thickness is uniquely defined if a_{ef} and w are known (see Appendix B).

[66] Equations (54) and (55) form a nonlinear system of two algebraic equations, having two unknowns (a_{ef} and w). Standard methods and programs are available for the solution of such problems. However, taking into account the specific form of equation (54), the exclusion method is used. This allows a single transcendent equation with one unknown (a_{ef}) to be formulated. It follows from equation (52) that

$$\tau_1 = \frac{4(t_1^{-1}(a_{ef}) - \alpha)}{3(1 - g_1(a_{ef}))}. \quad (56)$$

[67] On the other hand, the optical thicknesses τ_1 is related to the liquid water path w and the effective radius of droplets by the following equations (see Appendix B):

$$\tau_1 = w \bar{\sigma}_{ext}(\lambda_1, a_{ef}), \quad (57)$$

where $\bar{\sigma}_{ext} = \sigma_{ext}^*/\rho$, ρ is the density of water and σ_{ext}^* is given by equation (B3). We have from equations (56) and (57):

$$w = \frac{4\rho(t_1^{-1}(a_{ef}) - \alpha)}{3\sigma_{ext}^*(\lambda_1, a_{ef})(1 - g_1(a_{ef}))}, \quad (58)$$

where the dependence of functions on the value of the effective radius is explicitly noted. The value of t_1 is obtained from equation (54) (see also equations (50) and (51)). Thus, one unknown parameter (w) is expressed in terms of another parameter (a_{ef}).

[68] The substitution of equation (58) into equation (55) yields a single transcendent equation for the determination of the effective radius of droplets in a cloud. The equation obtained can be easily solved numerically. In particular, we use the standard subroutine *zbrent* described by *Press et al.* [1992]. This subroutine relies upon the Brent's method of finding roots of the function [*Brent*, 1973]. The obtained value of a_{ef} is used to calculate the optical thickness via equation (56). The liquid water path is determined from equation (58). This concludes the two-channel algorithm description for the determination of cloud parameters.

[69] Note that the subroutine *zbrent* performs the root search with a high speed. In practical terms, the speed is close to the speed of calculating an expression, consisting of ordinary elementary functions. The results are obtained immediately in real time. In this sense, we can drop the word "semi" from the title of our paper and treat our algorithm as a *truly* analytical inversion procedure, which is a surprising result, taking into account well-developed multiple light scattering in a cloud and large size of droplets. On the other hand, namely these two conditions allowed us to develop the algorithm.

[70] The algorithm proposed is extremely simple, robust, and fast. Moreover, the insight in the factors involved and equations presented can be of help for the general cloud optical studies, not necessarily related to the inverse problem. It could be also of interest to compare results of our retrieval procedure with other methods (and simultaneously with in situ measurements) for real cloud fields. We expect that, owing the complexity of cloud fields and all uncertainties involved [*Pincus et al.*, 1995], the method presented here will have in the end an accuracy similar to that obtained using the exact radiative transfer equation. This is mostly due to the fact that the notion "exact" is often (if not always) not relevant in studies of complex time and space-dependent fields of geophysical parameters.

[71] We would like to make one more remark. In some cases it is highly desirable to minimize the influence of generally unknown and potentially significant surface reflection. This is achieved by making both measurements in the infrared region of the electromagnetic spectrum [*Platnick et al.*, 2001]. Then equation (54) becomes:

$$\begin{aligned} \hat{R}_1 = {} & R_\infty^0 \exp(-y_1(1 - cy_1)u) - \left[\exp(-x_1 - y_1) - \frac{A_1 t_1}{1 - A_1 r_1}\right] \\ & \cdot t_1 K_0(\mu) K_0(\mu_0). \end{aligned} \quad (59)$$

where values of t_1, r_1, x_1, y_1 have the same meaning as in equation (55), but for another wavelength. The only difference is that the wavelength λ_1 is now in the near-infrared range of the electromagnetic spectrum.

[72] The retrieval procedure is based on the solution of two nonlinear equations (55) and (59) in this case. This can be easily performed numerically. It should be stressed, however, that the sensitivity of the reflection function in the infrared to the liquid water path is low. This is due to the fact that the function

$$\Omega(\mu, \mu_0, \varphi, \tau) = R_\infty(\mu, \mu_0, \varphi) - \hat{R}_1(\mu, \mu_0, \varphi, \tau) \qquad (60)$$

approaches zero with the increase of τ more rapidly in the infrared than it does in visible (see Figure 3a). This also means that the second term in equation (55) can be omitted in this case. This allows us to find the value of the cloud droplet effective radius for optically thick clouds with unknown values of the cloud optical thickness.

3.3. The Error Propagation Study

[73] The influence of various possible errors and uncertainties on the retrieved values of a_{ef} and τ needs to be investigated. This was done by many authors [*King*, 1987; *Rossow et al.*, 1989; *Pincus et al.*, 1995; *Asano et al.*, 2000]. However, for the sake of completeness, we need to revisit this issue.

[74] Let us consider first of all the one-channel algorithm, where all calculations can be done analytically [*King*, 1987]. In particular, we have the following result for the optical thickness as a function of the measured reflection function $\hat{R}$:

$$\tau = \frac{1}{b}\left[\frac{u}{v} - \frac{A}{1-A} - \alpha\right], \qquad (61)$$

where

$$b = \frac{3}{4}(1-g) \qquad (62)$$

and

$$v = 1 - \frac{\hat{R}_1}{R_\infty^0}. \qquad (63)$$

We have used equations (56) and (50), omitting index "1" for the sake of simplicity. The viewing function u is defined by equation (29), A is the surface albedo, and α is given by equation (11). It follows from equation (61) that the uncertainty in τ can be presented by the following equation:

$$\Delta\tau = \frac{\partial\tau}{\partial A}\Delta A + \frac{\partial\tau}{\partial v}\Delta v + \frac{\partial\tau}{\partial u}\Delta u + \frac{\partial\tau}{\partial b}\Delta b, \qquad (64)$$

where

$$\frac{\partial\tau}{\partial A} = -\frac{1}{b(1-A)^2}, \frac{\partial\tau}{\partial v} = -\frac{u}{bv^2}, \frac{\partial\tau}{\partial u} = \frac{1}{bv}, \frac{\partial\tau}{\partial b} = -\frac{\tau}{b}. \qquad (65)$$

Similar equations were derived earlier by *King* [1987]. The analysis of equations (64) and (65) allows to make the following conclusions:

1. The error of the determination of the optical thickness increases with the value of albedo as $(1-A)^{-2}$. In particular, $\frac{\partial\tau}{\partial A} \to \infty$ as $A \to 1$. This implies that it is impossible to find the optical thickness of any optically thick nonabsorbing cloud at $A = 1$. The physical grounds for such an effect are quite simple and will be discussed now. All photons transmitted by the cloud are reflected back to the cloud by the reflection from the underlying surface and then they return back to outer space. Thus, the value of the reflection function is that of a semiinfinite medium, which by definition does not depend on the optical thickness. The same result follows from equation (14) at $A = 1$. This makes it extremely difficult to retrieve the cloud optical thickness over white surfaces (e.g., snow, ice, and underlying cloud layers with high light reflectance) in the visible [*Platnick et al.*, 2001]. To avoid this problem one should make measurements in infrared or even microwave regions of the electromagnetic spectrum, where the albedo of natural underlying surfaces is low and atmospheric emission is high. It should be pointed out, however, that the value of the reflection function as a function of the optical thickness in the infrared region of the electromagnetic spectrum reaches a saturation value quite rapidly due to the high values of light absorption (see Figure 3a). This also makes it difficult to retrieve the optical thickness of thick clouds from measurements in infrared channels.

2. We have as $\tau \to \infty$: $R \to R_\infty$ and $v \to 0$. Note that the uncertainty in the retrieved value of the optical thickness due to the uncertainty in the value of v increases as v^{-2} as $v \to 0$. This makes it impossible (see equation (65) for $\frac{\partial\tau}{\partial v}$) to derive the optical thickness of extremely thick clouds with $\tau \geq \tau_{max}$. The upper limit of the optical thickness τ_{max} depends on many factors, including the surface albedo A, the maximal relative error of measurements δ, the observation geometry, the solar zenith angle and the value of the asymmetry parameter g. Let us define the value of the upper theoretical boundary of the optical thickness τ_{max}, which can be retrieved in principle from the reflection function measurements in the optical range by the following equation: $t(\tau_{max}) = \delta$, where the global transmittance t is given by equation (7). Clearly, the value of τ cannot be obtained for $\tau \geq \tau_{max}$ from reflection measurements in visible. Choosing the value of $g = 0.85$ and the error of measurements $\delta = 0.05$, we obtain that $\tau_{max} = 168$. The actual optical thickness of clouds is usually within the interval of 5–120 with the most frequently occurring value of around 30 [*Trishchenko et al.*, 2001]. So one can assume that the optical method of the cloud optical thickness determination does not have limits for large τ in practical terms. However, this is not true [*Pincus et al.*, 1995]. In particular, our estimation of τ_{max} was performed for black underlying surfaces. Actually, the maximal optical thickness τ_{max} depends on the surface albedo. It is smaller for larger surface albedos. It is smaller at smaller solar zenith angles (at nadir observation) due to larger contribution of multiple scattering in this case [*Pincus et al.*, 1995]. Actually, our estimation of τ_{max} should be substituted by $\tau_{max} - \Delta\tau$ where [*Zege et al.*, 1991] $\Delta\tau = \frac{4A}{3(1-g)(1-A)}$ for a nonzero surface albedo. We see that the actual value of the maximal optical thickness is negative at A close to 1. So it cannot be retrieved as it was discussed before. Values of A could reach 0.97 for snow surfaces. Then we have, assuming that $g = 0.85$: $\Delta\tau = 116$. This means that the actual maximal cloud optical thickness, which can be retrieved over snow areas in

visible is around 50. Actually, due to other uncertainties [*Pincus et al.*, 1995], it is even smaller.

3. Clearly, one can use infrared measurements in this case. The albedo of the snow surface is quite low in the infrared. However, another problem arises: light absorption by water cloud itself, which increases the cloud reflection function saturation rate. So one should use even larger wavelengths to avoid problems, which occur in the optical band (e.g., microwave cloud sounding from satellites).

4. The uncertainty in τ due to the uncertainty in the value of u is proportional to v^{-1} (see equation (65)). Therefore, it increases as $v \to 0$. This makes it important to have an accurate approximation for the viewing function u (see equation (29)) for the case of thick clouds.

5. The uncertainty in τ due to the uncertainty in the value of b is proportional to τ/b (see equation (65)). Thus, it is more important for larger values of the reduced optical length τ/b than for smaller ones. Larger values of g result in larger uncertainties in the optical thickness determination.

[75] Let us consider now the uncertainties in the retrieved parameters in the two-channel algorithm. Unfortunately, it is more difficult to do analytically. So we study this case using the numerical approach. The reflection function of a water cloud having a_{ef} = 10 μm, τ = 10, ϑ_0 = 49°, ϑ = 7°, φ = 0° and λ_1 = 0.65 μm, λ_2 = 1.55 μm is first calculated with the doubling-adding radiative transfer code. Then we introduce the error of measurements δ in both channels and retrieve values of a_{ef}, τ, using the algorithm, described in the previous section. Results are presented in Figure 4. As expected, the error of retrieval Δ increases with the value of δ. The value of Δ is not zero at $\delta = 0$ due to the approximations made in the formulae used in the inversion scheme. The error of retrieval is less than 10% for Δ = 5%, which is not untypical for satellite radiometric measurements. Note that the observation angle in this example is not exactly zero. However, the accuracy of retrieval is quite high. It suggests that equation (5) with b_1 = 1.48, b_2 = 7.76 can be used at other than nadir observation angles, providing that $\cos\vartheta_0 \approx 1$. The modification of equation (5) to account for arbitrary observation geometries will be considered in a separate publication.

[76] The second example is presented in Figure 5. For this case the value of δ is assumed to be equal to 5% and the influence of the optical thickness on the retrieval accuracy is investigated. One can see that the retrieval of τ for the case of larger optical thicknesses is more difficult. This is due to the reflection function being nearly independent of the thickness of a cloud at large τ (the limit of a semi-infinite medium) as discussed above.

[77] The error of the effective size retrieval initially increases with the value of τ. However, it approaches a finite value of approximately 20% independently of the optical thickness τ. This result is also easily understood. Indeed, equation (55) transforms into equation (32) as $\tau \to \infty$. The latter does not depend on the optical thickness. The error in this case can be retrieved analytically from equation (32). This is due to the fact that the two-channel algorithm is reduced to a one-channel algorithm (but for the effective radius of droplets determination). Namely, we have:

$$y = \frac{1}{u}\ln\frac{R_\infty^0}{R_\infty}, \tag{66}$$

where we neglected the value of c for the sake of simplicity (see equation (32)). On the other hand, it follows from equation (48):

$$y = \Xi\sqrt{\kappa a_{ef}}, \tag{67}$$

where Ξ = 6. Thus, it follows from equations (66) and (67):

$$a_{ef} = \frac{1}{\kappa\eta^2}\ln^2\frac{R_\infty^0}{R_\infty}, \tag{68}$$

where $\eta = \Xi u$. Therefore, we obtain for the uncertainty in a_{ef}:

$$\Delta a_{ef} = \frac{\partial a_{ef}}{\partial\kappa}\Delta\kappa + \frac{\partial a_{ef}}{\partial\eta}\Delta\eta + \frac{\partial a_{ef}}{\partial Q}\Delta Q, \tag{69}$$

where $Q = R_\infty^0/R_\infty$ and

$$\frac{\partial a_{ef}}{\partial\kappa} = -\frac{a_{ef}}{\kappa}, \frac{\partial a_{ef}}{\partial\eta} = -\frac{2a_{ef}}{\eta}, \frac{\partial a_{ef}}{\partial Q} = \frac{2a_{ef}}{Q\ln Q}. \tag{70}$$

From equations (69) and (70), the following can be summarized:

1. The relative error of the retrieval of the effective radius is equal (with opposite sign) to the error with which the absorption coefficient of water is known (at $\Delta\eta = \Delta Q = 0$). The value of $\Delta\kappa/\kappa$ is of the order of several percent, depending on the a priori unknown temperature of droplets [*Kuo et al.*, 1993; *Asano et al.*, 2000]. Note that the value of κ can be also modified by the presence of soot or aerosol particles trapped inside a droplet. This is a typical situation, e.g., over large industrial urban areas and cities. Obviously, the concentration of impurities also plays a role. This might well explain a discrepancy (constant shift of 5%) between satellite retrieved data for the effective radius and that obtained from in situ measurements [*Nakajima et al.*, 1991]. In situ measurements were performed using the laser diffractometer [*Nakajima et al.*, 1991] and the results, therefore, are largely insensitive to the value of the absorption coefficient. This is due to the fact that the information on the size of particles is obtained from the analysis of the diffraction pattern. This pattern almost entirely depends on the geometrical characteristics of droplets (primarily, on their diameter or droplet size distribution in the measured volume). This is, of course, not the case for the reflection function, which depends on the product κa_{ef} (see equation (48)).

2. The relative error of the retrieval of the effective radius of droplets is two times larger than (but with opposite sign) the error of the function $\eta = \Xi u$ (at $\Delta\kappa = \Delta Q = 0$). The error of the function $\eta = \Xi u$ results primarily from error in the approximate equation for the function $R_\infty^0(\mu, \mu_0, \varphi)$, which is approximately of 2%. This alone yields a uncertainty in the retrieved value of the effective radius of 4%.

3. It follows for the relative error of the effective radius determination at $\Delta\kappa = \Delta\eta = 0$:

$$\frac{\Delta a_{ef}}{a_{ef}} = P\frac{\Delta Q}{Q}, \tag{71}$$

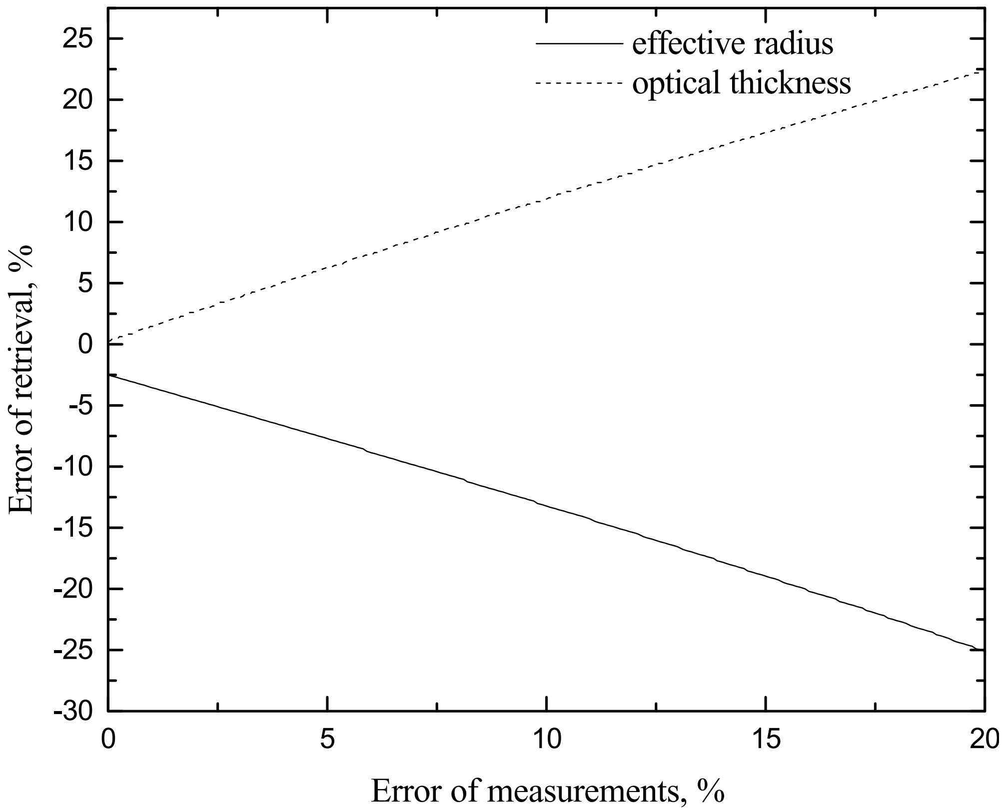

Figure 4. The dependence of the error of retrieval of a_{ef} and τ on the error of measurements Δ at $\vartheta_0 = 49°$, $\vartheta = 7°$, $\varphi = 0°$, $\lambda_1 = 0.65$ μm, $\lambda_2 = 1.55$ μm. It was assumed that $a_{ef} = 10$ μm and $\tau = 10$ at $\lambda = 0.65$ μm.

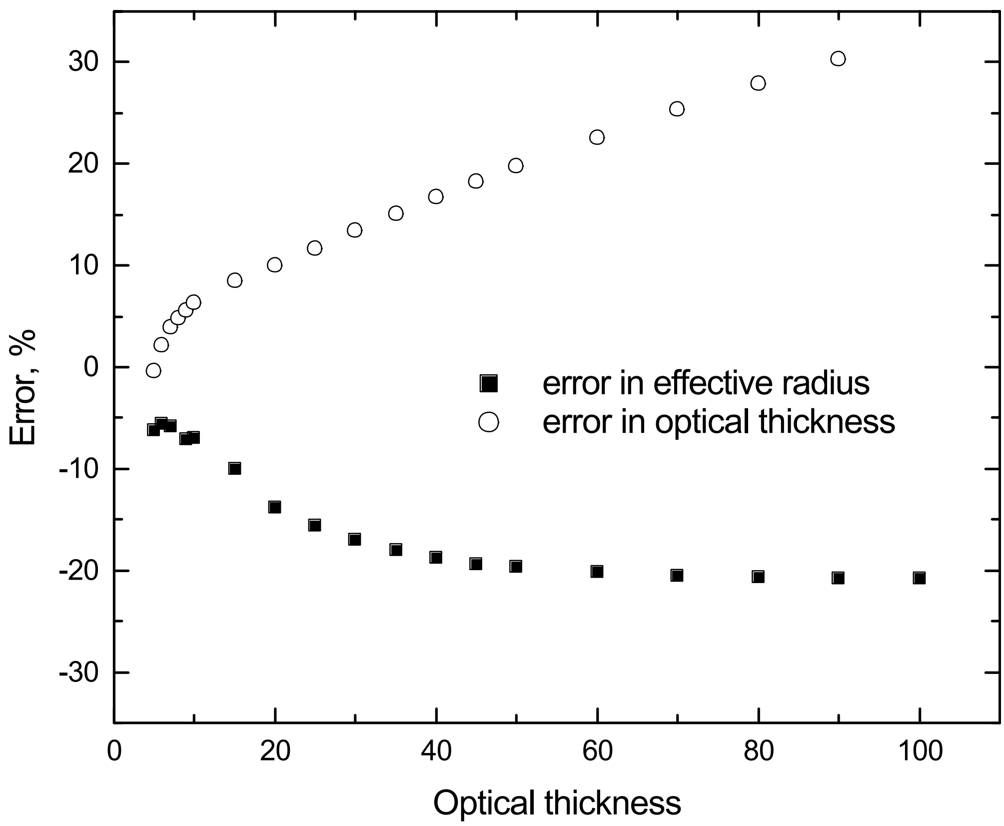

Figure 5. The dependence of the error of retrieval of a_{ef} and τ on the optical thickness τ at $a_{ef} = 6$ μm, $\vartheta_0 = 49°$, $\vartheta = 7°$, $\vartheta = 0°$, $\lambda_1 = 0.65$ μm, $\lambda_2 = 1.55$ μm, and $\delta = 5\%$.

where $P = 2\ln^{-1}Q$ is the error amplification coefficient. This coefficient is equal to infinity at $Q = 1$ as one can expect. It follows from our calculations that $Q = 1.5$ at $a_{ef} = 6$ μm, $\lambda = 1.55$ μm, $\vartheta_0 = 49°$, $\vartheta = 7°$ and $\varphi = 0°$. This means that $P \approx 4$ for this case and, correspondingly (see equation (71)) $\frac{\Delta Q}{Q} = 5\%$ at $\frac{\Delta Q}{Q} = 5\%$, which is close to the asymptotical value, determined numerically (see Figure 5 for the value of $\frac{\Delta a_{ef}}{a_{ef}}$ as $\tau \to \infty$). This confirms our calculations.

[78] In our discussion we completely omitted other sources of uncertainties like the imperfect knowledge of the atmospheric state, the in principle unknown cloud thermodynamic state, and the influence of possible subpixel cloud variability. Excellent reviews of these and other relevant issues, however, are available elsewhere [*Rossow et al.*, 1989; *Kobayashi*, 1993; *Cahalan et al.*, 1994; *Pincus et al.*, 1995; *Wang and King*, 1997; *Asano et al.*, 2000].

4. Conclusions

[79] Modern satellite cloud retrieval algorithms use either the lookup table approach or the classical asymptotic theory. The classical asymptotical theory is valid only for optically thick light scattering layers ($\tau \geq 10$). Clearly, both approaches converge as $\tau \to \infty$. In particular, *King* [1987] has shown that the difference between forward model results produced by two methods is below 1% at $\tau \geq 9$. This difference is completely negligible for all practical purposes. Note that most of the radiative transfer solvers also have numerical errors, which may reach 1% in some particular cases.

[80] Thus, there is no need to apply the exact radiative transfer equation and, therefore, conventional lookup table approaches to the cloud satellite retrievals for cases of optically thick cloudy media. For optically thin clouds, however, the application of the lookup table approach is not avoidable.

[81] The classical asymptotic theory offers a great simplification of the cloud inverse problem solution and should be used in the analysis of all scenes where optically thick clouds are present. It should be stressed, however, that asymptotic formulae (see equation (15)) do not provide the analytical solution of the radiative transfer equation in terms of elementary functions. Their application is not simple. In particular, one has to solve a number of integral equations to find auxiliary functions and parameters involved in the main result of the asymptotic theory, given by equation (15) [*Nakajima and King*, 1992].

[82] Asymptotic equations are valid at the arbitrary value of the single scattering albedo. The question arises whether it is possible to simplify these equations to account for a weak absorption of light in real terrestrial clouds (at least up to $\lambda = 2.3$ μm). The answer to this question is positive. To show this was the main idea of this paper. We also show the possibility to apply the developed scheme to the cloud inverse problem solution. Of course, obviously, this is not the only area of applicability of the equations obtained. We are currently working on generalizations of these equations for the case of inhomogeneous media and non-Lambertian surface reflectances. Other applications (e.g., to ice, snow, and foam optics) are also possible. Detailed studies of the accuracy of equations derived and their generalizations for smaller τ are given elsewhere [*Kokhanovsky and Rozanov*, 2003]. In particular, the error is less than 3% at $\tau \geq 8$ for cases presented in Figure 3a.

[83] Our method has a generally lower accuracy than a conventional asymptotic theory method as far as a forward modeling is concerned. However, it does not automatically mean that it will produce larger retrieval errors dealing with measurements performed in the terrestrial atmosphere. Indeed, errors of the modified asymptotic theory appear to be smaller than measurement uncertainties, not to mention a fundamental problem of partially cloud covered pixels or pixels with inhomogeneous cloud fields. This problem will be of a special importance, for a Scanning Imaging Absorption Spectrometer for Atmospheric Chartography (SCIAMACHY), launched on 1 March 2002 on board of the ENVIronmental SATellite (ENVISAT) [*Bovensmann et al.*, 1999]. The algorithm described here is specifically designed for this instrument, which has an extremely wide field of view (approximately, 30 × 60 km, depending on the wavelength). Obviously, in this case uncertainties other than differences between modified and conventional forms of asymptotic solutions will dominate the retrieval accuracy. We plan to discuss these issues, however, in our next publication.

Appendix A: The Phase Function

[84] Phase functions of water clouds at $\lambda = 0.65$ μm are presented in Figure A1. They have been obtained assuming the gamma particle size distribution

$$f(a) = Da^6 e^{-9a/a_{ef}}, \tag{A1}$$

where $D = const$ and the effective radius a_{ef} was changed from 4 to 20 μm. It is a complex task to model curves in Figure A1 with simple analytical equations.

[85] It should be stressed, however, that for most of cases the third term in the nominator of equation (5) ($p(\theta)$) is much smaller than the first and second terms. Thus, even the comparatively large error in the phase function $p(\theta)$ will not influence the reflection function $R^0_\infty(\vartheta, \vartheta_0, \varphi)$ in equation (5) very much. This follows from Figure 1 as well. Thus, we will neglect the dependence of the phase function on the size of droplets and use the following approximation, obtained by the parametrization of computations with the exact Mie theory:

$$p(\theta) = \xi e^{-\sigma} + \sum_{i=1}^{5} b_i e^{-\beta_i(\theta-\theta_i)^2}, \tag{A2}$$

where θ is the scattering angle in radians, $\xi = 17.7$, $\sigma = 3.9$ and constants b_i, β_i, θ_i are presented in Table A1. The accuracy of this approximation can be estimated from Figure A1.

Appendix B: Integral Light Scattering Characteristics

[86] Integral light scattering and absorption characteristics of water clouds can be found with following equations [*Kokhanovsky*, 2001]:

$$\sigma_{ext} = \sigma^*_{ext} C_v, \sigma_{abs} = \sigma^*_{abs} C_v, \tag{B1}$$

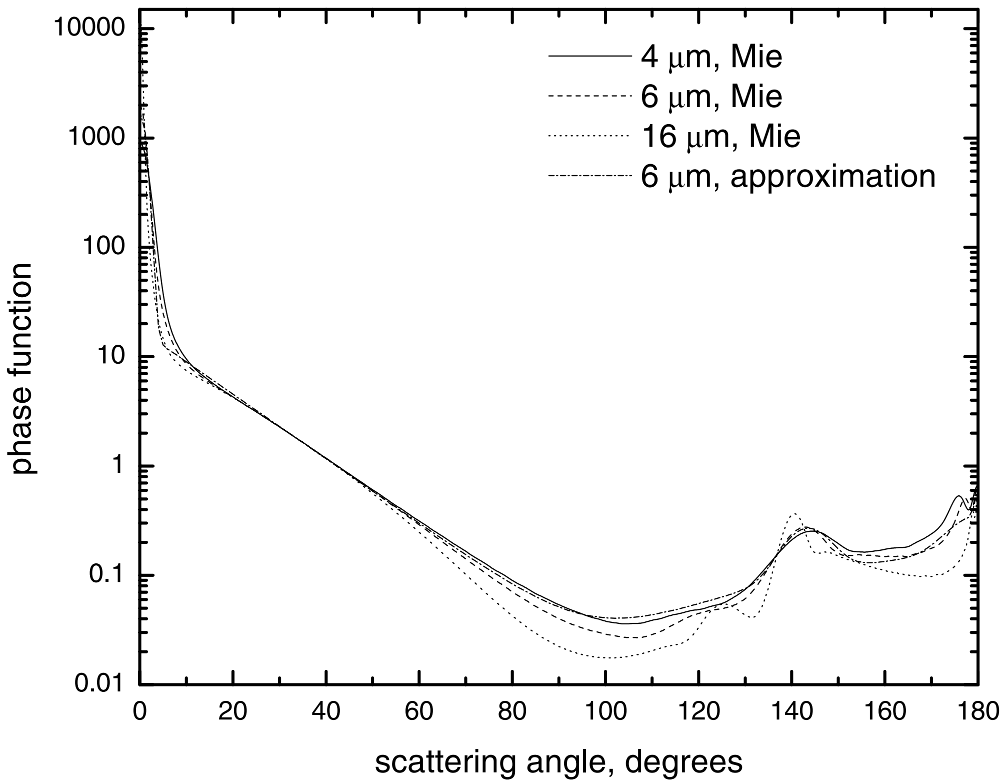

Figure A1. Phase functions of water clouds at different values of a_{ef} obtained with the Mie theory and approximation (A2).

$$1 - g = 0.12 + 0.5\left(ka_{ef}\right)^{-2/3} - 0.15\kappa a_{ef}, \tag{B2}$$

where $k = 2\pi/\lambda$, λ is the wavelength, a_{ef} is the effective size of droplets, $\kappa = 4\pi\chi/\lambda$, χ is the imaginary part of the refractive index of water $C_v = N\langle V\rangle$, is the volumetric concentration of droplets, N is number of droplets in a unit volume of a cloud, $\langle V\rangle$ is the average volume of a droplet in a unit volume of a cloudy medium, g is the asymmetry parameter, σ_{ext} and σ_{abs} are extinction and absorption coefficients. The values of σ^*_{ext} and σ^*_{abs} are given by [*Kokhanovsky*, 2001]:

$$\sigma^*_{ext} = \frac{1.5}{a_{ef}}\left(1 + \frac{1.1}{\left(ka_{ef}\right)^{2/3}}\right), \tag{B3}$$

$$\sigma^*_{abs} = \frac{5\pi\chi\left(1 - \kappa a_{ef}\right)}{\lambda}\left(1 + 0.34\left(1 - \exp\left(-\frac{8\lambda}{a_{ef}}\right)\right)\right). \tag{B4}$$

It follows from equations (B1) and (B3) for the ratio of extinction coefficients at two wavelengths:

$$\Phi = \frac{1.1 + \varsigma_2^{2/3}}{1.1 + \varsigma_1^{2/3}}, \tag{B5}$$

where, $\varsigma_j = \frac{2\pi a_{ef}}{\lambda_j}$, j = 1,2. Note that we have for large values of $\zeta_j \to \infty$: $\Phi \to 1$.

[87] The optical thickness is given by:

$$\tau = \sigma_{ext}L, \tag{B6}$$

where L is the geometrical thickness of a cloud. It follows from equations (B6), (B1), and (B3):

$$\tau = \bar{\sigma}_{ext}w, \tag{B7}$$

where $w = \rho C_v L$ is the liquid water path, ρ is the density of water $\bar{\sigma}_{ext} = \sigma^*_{ext}/\rho$. Note that values of $\bar{\sigma}_{ext}$ and σ^*_{ext} numerically coincide if a_{ef} is expressed in μm and ρ in g/m^3. Then w in equation (B7) is given in g/m^2. The accuracy of equations (B1)–(B4) has been studied by *Kokhanovsky and Zege* [1995, 1997] and *Kokhanovsky* [2001]. It is better than 5–8% at λ < 2.2 μm.

[88] If higher accuracy is needed one can use the direct parametrization of the Mie calculations. We obtain with the

Table A1. Parameters b_i, β_i, and θ_i

i	b_i	β_i	θ_i
1	1744.0	1200.0	0.0
2	0.17	75.0	2.5
3	0.30	4826.0	π
4	0.20	50.0	π
5	0.15	1.0	π

Table B1. Parameters c_i for Different Wavelengths λ

λ (μm)	c_0	c_1	c_2	c_3	c_4
0.6457	0.1121	0.5118	0.8997	0.0	0.0
0.8590	0.1115	0.4513	1.2719	0.0	0.0
1.239	0.1095	0.4198	1.5796	0.0	0.0
1.549	0.0608	2.465	−32.98	248.94	−636
λ (μm)	d_0	d_1	d_2	d_3	d_4
1.239	1.779	−0.0068	4.94E−5	−1.425E−7	0
1.549	1.671	0.0025	−2.365E−4	2.861E−6	−1.05E−8

accuracy better than 1% at selected wavelengths, which are almost free of gaseous absorption:

$$1-g=\sum_{n=0}^{4} c_n\left(ka_{ef}\right)^{-2n/3}, \quad (B8)$$

$$\sigma_{abs}=\frac{4\pi\chi}{\lambda}c_v\sum_{n=0}^{4} d_n\left(ka_{ef}\right)^{n}, \quad (B9)$$

where constants c_n, d_n, are presented in Table B1 at λ = 0.6457, 0.8590, 1.239 and 1.549 μm. There is no need to modify equation (B3) due to the high accuracy of this equation in the spectral range under consideration.

[89] At larger wavelengths it is easier to make parametrizations of parameters y and $z = x/w$ instead of σ_{ext}, σ_{abs} and $1 - g$. In particular, it follows at $\lambda = 2.3$ μm:

$$y = 0.24206 + 0.02524x_{ef} - 1.4197 \cdot 10^{-4}x_{ef}^2, \quad (B10)$$

$$z = 0.02008 - 0.54709x_{ef}^{-2/3} + 7.53062x_{ef}^{-4/3} - 15.1524x_{ef}^{-2}. \quad (B11)$$

Note that the value of y is dimensionless. The dimension of z coincides with that of the liquid water path w.

[90] **Acknowledgments.** This work has been made possible by support of the Institute of Environmental Physics and Remote Sensing, the University of Bremen, the European Union Research Programme, the European Space Agency, the German Ministry of Research and Education (BMBF), and the German Space Agency (DLR). This work is a part of the preparation for the retrieval of cloud parameters from the SCIAMACHY [*Bovensmann et al.*, 1999] data.

References

Arking, A., and J. D. Childs, Retrieval of clouds cover parameters from multispectral satellite images, *J. Appl. Meteorol.*, *24*, 323–333, 1985.
Asano, S., et al., Effects of aerosols on retrieval of the microphysical properties of water clouds from the airborne solar spectral reflectance measurements, *Proc. SPIE*, *4150*, 208–216, 2000.
Bovensmann, H., et al., SCIAMACHY: Mission objectives and measurement modes, *J. Atmos. Sci.*, *56*, 127–150, 1999.
Brent, R. P., *Algorithms for the Minimization without Derivatives*, Prentice-Hall, Old Tappan, N. J., 1973.
Bucholtz, A., Rayleigh-scattering calculations for the terrestrial atmosphere, *Appl. Opt.*, *34*, 2765–2773, 1995.
Cahalan, R. F., et al., The albedo of fractal stratocumulus clouds, *J. Atmos. Sci.*, *51*, 2434–2455, 1994.
Deschamps, P.-Y., et al., The POLDER Mission: Instrument characteristics and scientific objectives, *IEEE Trans. Geosci. Remote Sens.*, *32*, 598–614, 1994.
Feigelson, E. M., (ed.), *Radiation in a Cloudy Atmosphere*, 280 pp., Gidrometeoizdat, St. Petersburg, Russia, 1981.
Goloub, P., et al., Cloud thermodynamical phase classification from the POLDER spaceborne instrument, *J. Geophys. Res.*, *105*, 14,747–14,759, 2000.
Germogenova, T. A., Some formulas to solve the transfer equation in the plane layer problem, in *Spectroscopy of Scattering Media*, edited by B. I. Stepanov, pp. 36–41, AN BSSR, Minsk, 1963.
Han, Q., et al., Near global survey of effective droplet radii in liquid water clouds using ISCCP data, *J. Clim.*, *7*, 465–497, 1994.
King, M. D., A method for determining the single scattering albedo of clouds through observation of the internal scattered radiation field, *J. Atmos. Sci.*, *38*, 2031–2044, 1981.
King, M. D., Determination of the scaled optical thickness of clouds from reflected solar radiation measurements, *J. Atmos. Sci.*, *44*, 1734–1751, 1987.
King, M. D., et al., Remote sensing of cloud, aerosol, and water vapour properties from the moderate resolution imaging spectrometer (MODIS), *IEEE Trans. Geosci. Remote Sens.*, *30*, 2–27, 1992.
Kobayashi, T., Effects due to cloud geometry on biases in the albedo derived from radiance measurements, *J. Clim.*, *6*, 120–128, 1993.
Kokhanovsky, A. A., *Light Scattering Media Optics: Problems and Solutions*, 2nd edition, Springer-Verlag, New York, 2001.
Kokhanovsky, A. A., Simple approximate formula for the reflection function of a homogeneous semi-infinite turbid medium, *J. Opt. Soc. Am. A Opt. Image Sci.*, *19*, 957–960, 2002a.
Kokhanovsky, A. A., Reflection and polarization of light by semi-infinite turbid media: Simple approximations, *J. Colloid Interface Sci.*, *251*, 429–433, 2002b.
Kokhanovsky, A. A., and E. P. Zege, Local optical parameters of spherical polydispersions: Simple approximations, *Appl. Opt.*, *34*, 5513–5519, 1995.
Kokhanovsky, A. A., and E. P. Zege, Physical parametrization of local optical characteristics of cloudy media, *Izv. Russ. Acad. Sci. Atmos. Oceanic Phys., Engl. Transl.*, *33*, 209–218, 1997.
Kokhanovsky, A. A., T. Nakajima, and E. P. Zege, Physically-based parametrizations of the shortwave radiative characteristics of weakly absorbing optically thick media: Application to liquid water clouds, *Appl. Opt.*, *37*, 4750–4757, 1998.
Kokhanovsky, A. A., and V. V. Rozanov, The reflection function of optically thick weakly absorbing turbid layers: A simple approximation, *J. Quant. Spectrosc. Radiat. Transfer*, *77*, 167–175, 2003.
Kondratyev, K. Ya., and V. I. Binenko, *Impact of Cloudiness on Radiation and Climate*, Gidrometeoizdat, St. Petersburg, Russia, 1984.
Kuo, L., et al., Refractive indices of water and ice in the 0.65- to 2.5-μm range, *Appl. Opt.*, *32*, 3531–3540, 1993.
Liou, K. N., *Radiation and Cloud Processes in the Atmosphere*, Oxford Univ. Press, New York, 1992.
Loeb, N. G., and R. Davies, Observational evidence of plane parallel model biases: Apparent dependence of cloud optical depth on solar zenith angle, *J. Geophys. Res.*, *101*, 1621–1634, 1996.
Loeb, N. G., and J. A. Coakley Jr., Inference of marine stratus cloud optical depths from satellite measurements: Does 1D theory apply?, *J. Atmos. Sci.*, *11*, 215–233, 1998.
Los, A., and P. G. Duynkerke, Microphysical and radiative properties of inhomogeneous stratocumulus: Observations and model simulations, *Q. J. R. Meteorol Soc.*, *126*, 3287–3307, 2000.
Minin, I. N., *Radiative Transfer Theory in Planetary Atmospheres*, Nauka, Moscow, 1988.
Mishchenko, M. I., J. M. Dlugach, E. G. Yanovitskij, and N. T. Zakharova, Bidirectional reflectance of flat, optically thick particulate layers: An efficient radiative transfer solution and applications to snow and soil surfaces, *J. Quant. Spectrosc. Radiat. Transfer*, *63*, 409–432, 1999.
Nakajima, T., and M. D. King, Determination of the optical thickness and effective particle radius of clouds from reflected solar radiation measurements, part I, Theory, *J. Atmos. Sci.*, *47*, 1878–1893, 1990.
Nakajima, T., and M. D. King, Asymptotic theory for optically thick layers: Application to the discrete ordinates method, *Appl. Opt.*, *31*, 7669–7683, 1992.
Nakajima, T., M. D. King, J. D. Spinhirne, and L. F. Radke, Determination of the optical thickness and effective particle radius of clouds from reflected solar radiation measurements, part II, Marine stratocumulus observations, *J. Atmos. Sci.*, *48*, 728–750, 1991.
Nakajima, T. Y., et al., Optimization of the Advanced Earth Observing Satellite II Global Imager channels by use of the radiative transfer calculations, *Appl. Opt.*, *37*, 3149–3163, 1998.
Pincus, R., et al., Uncertainty in cloud optical depth estimates made from satellite radiance measurements, *J. Clim.*, *8*, 1453–1462, 1995.
Platnick, S., Approximations for horizontal photon transport in cloud remote sensing problems, *J. Quant. Spectrosc. Radiat. Transfer*, *68*, 75–99, 2001.
Platnick, S., et al., A solar reflectance method for retrieving the optical thickness and droplet size of liquid water clouds over snow and ice surfaces, *J. Geophys. Res.*, *106*, 15,185–15,199, 2001.
Press, W. H., et al., *Numerical Recipes in Fortran: The Art of Scientific Computing*, 2nd edition, Cambridge Univ. Press, New York, 1992.
Rossow, W. B., Measuring cloud properties from space: A review, *J. Clim.*, *2*, 419–458, 1989.
Rossow, W. B., and R. A. Schiffer, Advances in understanding clouds from ISCCP, *Bull. Am. Meteorol. Soc.*, *80*, 2261–2287, 1999.
Rossow, W. B., et al., Global, seasonal cloud variations from satellite radiance measurements, part I, Sensitivity of analysis, *J. Clim.*, *2*, 419–458, 1989.
Rozenberg, G. V., Optical characteristics of thick weakly absorbing scattering layers, *Dokl. Acad. Nauk*, *145*, 775–777, 1962.
Rozenberg, G. V., *Twilight*, Plenum, New York, 1966.
Rozenberg, G. V., et al., The determination of optical characteristics of clouds from measurements of the reflected solar radiation using data from the Sputnik "KOSMOS-320", *Izv. Russ. Acad. Sci. Atmos. Oceanic Phys., Engl. Transl.*, *10*, 14–24, 1978.

Slingo, A., A GCM parametrization for the shortwave radiative properties of water clouds, *J. Atmos. Sci.*, *46*, 1419–1427, 1989.
Sobolev, V. V., *Light Scattering in Planetary Atmospheres*, Nauka, Moscow, 1972.
Sobolev, V. V., Integral relations and asymptotic expressions in the theory of radiative transfer, *Astrofizika*, *20*, 123–132, 1984.
Trishchenko, A. P., et al., Cloud optical depth and TOA fluxes: Comparison between satellite and surface retrievals from multiple platforms, *Geophys. Res. Lett.*, *28*, 979–982, 2001.
Van de Hulst, H. C., *Multiple Light Scattering: Tables, Formulas and Applications*, Academic, San Diego, Calif., 1980.
Wang, M., and M. D. King, Correction of Rayleigh scattering effects in cloud optical thickness retrievals, *J. Geophys. Res.*, *102*, 25,915–25,926, 1997.
Yanovitskij, E. G., *Light Scattering in Inhomogeneous Atmospheres*, Springer-Verlag, New York, 1997.
Zege, E. P., A. P. Ivanov, and I. L. Katsev, *Image Transfer through a Scattering Medium*, Springer-Verlag, New York, 1991.

H. Bovensmann, J. P. Burrows, A. A. Kokhanovsky, and V. V. Rozanov, Institute of Environmental Physics, University of Bremen, FB 1, P.O. Box 330440, Otto-Hahn-Allee 1, 28334 Bremen, Germany. (alexk@iup.physik.uni-bremen.de)

E. P. Zege, Institute of Physics, National Academy of Sciences of Belarus, 70 Skarina Avenue, 220072 Minsk, Belarus.